

## Regional Infant Brain Development: An MRI-Based Morphometric Analysis in 3 to 13 Month Olds

Myong-sun Choe<sup>1,2,3,5</sup>, Silvia Ortiz-Mantilla<sup>7</sup>, Nikos Makris<sup>3</sup>, Matt Gregas<sup>4</sup>, Janine Bacic<sup>4</sup>, Daniel Haehn<sup>1,6</sup>, David Kennedy<sup>3,8</sup>, Rudolph Pienaar<sup>1,5,6</sup>, Verne S. Caviness, Jr<sup>3</sup>, April A. Benasich<sup>7</sup> and P. Ellen Grant<sup>1,2,5,6</sup>

<sup>1</sup>Fetal-Neonatal Neuroimaging and Developmental Science Center, Children's Hospital Boston, <sup>2</sup>Division of Newborn Medicine, Department of Medicine, Children's Hospital Boston, <sup>3</sup>Department of Neurology, Center for Morphometric Analysis, Massachusetts General Hospital, <sup>4</sup>Clinical Research Program, Department of Neurology, Children's Hospital Boston, <sup>5</sup>Athinoula A. Martinos Center for Biomedical Imaging, Massachusetts General Hospital, and <sup>6</sup>Division of Neuroradiology, Department of Radiology, Children's Hospital Boston, Harvard Medical School, Boston, MA, USA <sup>7</sup>Department of Neuroscience, Rutgers, Center for Molecular and Behavioral Neuroscience, The State University of New Jersey, Newark, NJ, USA and <sup>8</sup>Child and Adolescent NeuroDevelopment Initiative (CANDI), Department of Psychiatry, University of Massachusetts Medical School, Worcester, MA, USA

Address correspondence to P. Ellen Grant, Fetal-Neonatal Neuroimaging and Developmental Science Center, Children's Hospital Boston, Harvard Medical School, Boston, MA, USA. Email: ellen.grant@childrens.harvard.edu

**Elucidation of infant brain development is a critically important goal given the enduring impact of these early processes on various domains including later cognition and language. Although infants' whole-brain growth rates have long been available, regional growth rates have not been reported systematically. Accordingly, relatively less is known about the dynamics and organization of typically developing infant brains. Here we report global and regional volumetric growth of cerebrum, cerebellum, and brainstem with gender dimorphism, in 33 cross-sectional scans, over 3 to 13 months, using  $T_1$ -weighted 3-dimensional spoiled gradient echo images and detailed semi-automated brain segmentation. Except for the midbrain and lateral ventricles, all absolute volumes of brain regions showed significant growth, with 6 different patterns of volumetric change. When normalized to the whole brain, the regional increase was characterized by 5 differential patterns. The putamen, cerebellar hemispheres, and total cerebellum were the only regions that showed positive growth in the normalized brain. Our results show region-specific patterns of volumetric change and contribute to the systematic understanding of infant brain development. This study greatly expands our knowledge of normal development and in future may provide a basis for identifying early deviation above and beyond normative variation that might signal higher risk for neurological disorders.**

**Keywords:** Brain development, Infant, MRI, Volumetric analysis

### Introduction

The human brain grows significantly during the first few years of life. The brain volume of neonates is 380 to 420 cm<sup>3</sup> (Huppi et al. 1998), which is only about one-fourth to one-third of its adult volume. Total cerebral volume at 2 to 4 weeks of age is ~36% and that at 1 year is ~72% of adult volume (Knickmeyer et al. 2008). At 3 years, total cerebral volume is approximately 80% of adult volume and reaches 90 to 92% at 9 years (range 7 to 11 years) (Caviness, Kennedy, Richelme, et al. 1996; Caviness, Kennedy, Bates, et al. 1996; Caviness, Meyer, et al. 1996). In fact, intracranial volume increases by about 300 mL between 3 months and 10 years (Pfefferbaum et al. 1994), with total cerebral volume peaking at 10.5 years in females and at 14.5 years in males (Lenroot et al. 2007).

High postnatal brain growth rates have been interpreted as an extension of fetal modes of growth into early infancy (Martin 1983). As a result of the dynamic orchestration of neuronal connectivity and the integration of neuronal activity, the infant, from the first days of life, begins to acquire increasingly complex motor and sensory skills as well as construct the neural substrates of cognitive function. The impact of differences in head growth across early development on later intelligence, using head circumference as a surrogate for brain volume, has been demonstrated. The brain volume a child achieves by the end of the first year is an important determinant of later intelligence; moreover, the growth in brain volume after the infancy period may not compensate for poorer earlier growth (Gale et al. 2006).

Structural magnetic resonance imaging (MRI) of pediatric brain development has been studied over the past 2 decades (Giedd and Rapoport 2010). Volumetric determination of brain sub-regions as well as cerebellum of myelinated brains in older children has been carried out in various studies based on MRI (Ostby et al. 2009; Tiemeier et al. 2010). The estimated regional cortical gray matter growth and cerebral asymmetry have been reported in the neonatal brain and that in 1 and 2 year olds (Huppi et al. 1998; Gilmore et al. 2007, 2011; Knickmeyer et al. 2008; Shi et al. 2011). However, morphometric analyses of brain subcortical regions during the first year of life have not yet been reported. Obtaining infant brain images is difficult due to technical reasons (e.g. head and body movements) and inherent features of the developing brain (immature pattern of magnetic resonance contrast due to incomplete myelination and dynamic changes in the contrast with age). These features make segmentation especially challenging for sub-cortical regions such as the caudate, putamen, globus pallidus, thalamus, hippocampus, and amygdala. Reliable techniques for segmenting these small regions are under development. Consequently, differential growth patterns of cerebral deep gray matter regions (caudate, putamen, globus pallidus, thalamus, hippocampus, and amygdala) during the very early stages of postnatal development have not yet been characterized.

Volumetric measures of cerebral deep gray matter regions in relation to a number of disorders such as developmental amnesia, autism, and attention deficit hyperactivity disorder (ADHD) have shown differences in older

children (Castellanos et al. 1996, 2002; Gadian et al. 2000; Isaacs et al. 2003; Wellington et al. 2006). However, no studies to date have reported predictive associations between volumetric measures of infant brain structures and such disorders, as no reliable method is available for obtaining such measures while the infant brain myelinates. Given the plasticity of the brain early in development, earlier detection of growth pattern abnormalities may allow improved outcomes through early intervention. In typically developing children, normal volumetric variability in infant brain regions has been related to behavioral outcomes. We recently reported significant and consistent correlations between amygdala size and language abilities. Children with larger right amygdala at 6 months had lower scores on expressive and receptive language measures at 2, 3, and 4 years (Ortiz-Mantilla et al. 2010), and lower metalinguistic abilities and phonological awareness at 5 years (Ortiz-Mantilla et al. in preparation). Development of a reliable method to accurately carry out segmentation of normally developing infant brain using 3-dimensional (3D) magnetic resonance images may give us a more accurate understanding of normal development, and help define pathology for infants at risk.

This paper is the first report to demonstrate developmental volumetric changes and differential growth in the infant brain, including global and local volumes across 3 to 13 months using a mostly cross-sectional design (33 brain scans of 3 to 4 month olds ( $n=5$ , males 2, females 3), 6 to 7 month olds ( $n=19$ , males 11, females 8), and 12 to 13 month olds ( $n=9$ , males 5, females 4)). We describe in detail our method for segmenting the sub-cortical brain structures in infants. Furthermore, we propose that during the first year of age, individual brain structures exhibit different volumetric changes and sexual dimorphism in the normally developing brain. To illustrate this differential growth, we have characterized the patterns of volumetric change for individual regions and modeled their growth across age as infants mature. We show that many structures demonstrate measurable differences in growth across time, as well as gender dimorphism.

## Methods

### Participants

Participants in this sample were part of a large, longitudinal study that aimed to establish developmental landmarks, including normative anatomic baselines and variation in brain development on MRI across the first 2 years of life. Twenty-seven full-term normally developing children were included in this study. The group consisted of 14 males and 13 females with 6 subjects measured at 2 time points. Five

**Table 1**  
Scan age and gender distribution

Age: months, weeks	N: male, female
3, 12 to 15	4: 2, 2
4, 17	1: 0, 1
6, 26 to 27	9: 5, 4
7, 28 to 30	10: 6, 4
12, 48 to 51	6: 4, 2
13, 52 to 55	3: 1, 2
Median: 7, 28	Total: 33: 18, 15

Note: Thirty-three scans of infant brain were obtained from 27 participants. Two repeated scans at 2 time points were obtained from 6 of the participants.

children were successfully scanned at both 6 and 12 months and 1 child at both 3 and 12 months, for a total of 33 brain scans (Table 1). The 33 brain scans include 3 to 4 month olds (12 to 17 week olds,  $n=5$ , males 2, females 3), 6 to 7 month olds (26 to 30 week olds,  $n=19$ , males 11, females 8), and 12 to 13 month olds (48 to 55 week olds,  $n=9$ , males 5, females 4), median 7 months, 28 weeks. All children were born healthy, full-term (39 to 42 weeks of gestation; mean = 40.42, median = 41 weeks) and ranged in weight from 2971 to 4649 g (mean = 3585.89 g, SD = 412.7). Most of the children were recruited between 2002 and 2005, from urban and suburban communities in New Jersey, through parenting group presentations, website advertising, and mailing lists for researchers at the Center for Molecular & Behavioral Neuroscience, at Rutgers University. An informed consent (approved by the Rutgers Human Subjects Board) that allowed the child to participate was signed by all parents prior to the child's inclusion in the study.

All infants included in this study had uneventful pre- and perinatal courses and were born into English monolingual families. There was no history of hearing dysfunction or recurrent episodes of otitis media. Participants were screened for first-degree and/or second-degree family history of language disorders, autism, autoimmune disease, seizures, and other neurological disorders as well as for allergies and asthma. This information was reviewed with the parent and additional information or clarification was obtained if needed. Socio-demographic data, as well as information about infant and maternal health, and obstetrical history were collected at the 6-month visit via parental questionnaire. Further follow-up questionnaires solicited additional infant health data at each subsequent visit. The parent's socioeconomic status (SES) was assessed by the Hollingshead Four-factor index (Hollingshead 1975). Infants came from families classified as middle-to-upper middle class (SES ranging from 32 to 66, mean = 55.81, SD = 8.9). Parents were compensated for their time and babies received a toy after their visit. Children visited the laboratory for testing at 3, 6, 12, 24, 36, 48, and 60 months. A supplemental questionnaire was used at each subsequent visit to make sure no "new" issues had arisen—for example with an older sibling. At each age a comprehensive battery of age-appropriate perceptual, cognitive, and language tests were administered over the course of 3 to 4 visits. Assessments were conducted by psychologists, speech language pathologists, and highly trained research assistants. In the study detailed here, we had strict exclusion criteria so we could obtain a normal sample. All study children scored within the normal range on this extensive neuropsychological battery.

### MR Image Acquisition

At 3, 6, or 12 months, one of the study visits was scheduled for late afternoon/early evening so that a nonsedated, naturally sleeping MRI could be more easily acquired. In the imaging suite, an attempt was made to replicate normal bedtime routines for the child by including soft lullaby music, a rocking chair, a crib, and any other objects or materials that might encourage sleep (for a detailed explanations of the scanning procedures, see Paterson et al. 2004; Liu et al. 2008; Raschle et al. 2012). All children were scanned with a 1.5 Tesla magnetic resonance system (General Electric Signa 5.X: GE 1.5 T Echospeed) during natural sleep without sedation.  $T_1$ -weighted, 3D spoiled gradient echo (SPGR) images were obtained using a quadrature adult head coil. The imaging parameters were as follows: TR/TE = 24/10 ms, flip angle = 30°, matrix = 256 × 256, bandwidth = 122, slice thickness = 1.2 to 1.5 mm, FOV = 250 mm, NEX = 1. Six of the children in this sample (4 males, 2 females) had successful MRIs at 2 age points for a total of 33 MRI scans.

### Morphometric Analysis

For the anatomic segmentation, the images were first positionally normalized and bias field corrected. After repositioning, a tri-linear interpolation method was used to resample the MR image dataset to a resolution of 1.0 mm in the newly defined, "normalized" coronal plane and 0.98 mm in the sagittal and axial planes for optimal visualization and subsequent segmentation (Filipek et al. 1991; Nishida et al. 2006). Images were then segmented in *CardViews*, a semi-

automated brain segmentation tool, using previously described highly reliable and reproducible segmentation methods and labeled to extract volumetric data (Nishida et al. 2006). These segmentations were performed according to the anatomic boundaries of Filipek et al. (1994) with minor modifications in our infant subjects. The investigator defines anatomical regions using the techniques explained below. The accuracy was confirmed by an expert neuroradiologist's (P.E.G.) review of every segmented image. These detailed computer-assisted semi-automated techniques of mature, fully myelinated brains have been developed at the Center for Morphometric Analysis (CMA), the Massachusetts General Hospital, since 1989 and extensively published (Rademacher and Galaburda 1992; Kennedy and Meyer 1994; Caviness, Kennedy, Richelme, et al. 1996; Caviness, Kennedy, Bates, et al. 1996; Caviness, Meyer, et al. 1996; Makris et al. 1999; Meyer et al. 1999). Nishida et al. at CMA extended this technique for the neonatal brain and developed a knowledge-based, reliable, and reproducible segmentation process for minimally myelinated brains, such as normative neonates (Nishida et al. 2006). In this paper, we further extend this technique to the infant brain as the myelination process unfolds (3 to 13 months).

The brains were segmented into the following regions: Cerebrum, brainstem, and cerebellum. The cerebrum was further segmented into cerebral cortex, cerebral white matter, and cerebral deep gray matter structures such as caudate nuclei, lentiform nuclei (putamen and globus pallidum), hippocampi, amygdalae, thalamci, and ventral diencephalon (VDC). The VDC was defined as a group of structures below the thalamus that generally cannot be distinguished from each other with standard MR images. This area includes the hypothalamus, mammillary body, subthalamic nuclei, substantia nigra, red nucleus, lateral geniculate nucleus, and medial geniculate nucleus. White matter areas such as the zona incerta, cerebral peduncle (crus cerebri), and the lenticular fasciculus are also included in this area (Filipek et al. 1989; Herbert et al. 2003; CMA 2004). The brainstem was then further segmented into midbrain, pons, and medulla and the cerebellum into cerebellar vermis and cerebellar hemispheres. Neuroanatomic segmentation was performed using the techniques of semi-automated intensity contour algorithms, signal intensity histogram distributions, and manual editing. Semi-automated intensity contour algorithms and signal intensity histogram distribution allows

for border definition as it defines the mid-point between the peaks of the bimodal distribution for any given region and its surrounding tissue (Worth, Makris, Caviness, et al. 1997; Worth, Makris, Meyer, 1997). Manual editing, as anatomically necessary, was made to complete the anatomic border. These manually guided boundaries were created in the coronal plane with placement guided by detailed knowledge of the regional anatomy (Fig. 1), reformations, and boundaries drawn on the sagittal and axial plane projected into the coronal plane.

Manual drawing is the most time-consuming process in segmentation; however, it is the most accurate technique to define anatomical boundaries in infant brain provided that the investigator has a highly detailed knowledge of the anatomy. Unlike in fully myelinated brain, intensity contour mapping often cannot detect accurate borders, especially of cerebral deep gray matter regions, due to incomplete myelination, low contrast, low signal-to-noise ratio, and motion effect, etc. The projection from the axial or sagittal to the coronal image reconstructs an anatomically more accurate form of the region in the coronal plane. Therefore, manual tracing including reference lines in the axial or sagittal planes is essential for accurate segmentation. Further details of these operations for fully myelinated brains are described elsewhere (Kennedy 1986; Kennedy and Nelson 1987; Caviness et al. 1989; Filipek et al. 1989, 1991; Filipek and Kennedy 1992; Kennedy and Filipek 1989).

In order to obtain visually accurate reproducible results, the previously described methods required the following modifications:

- (a) Amygdala–Hippocampus. The amygdala and hippocampus attach tightly to each other anteriorly in the temporal lobe, whereas the hippocampus rests beneath the floor of the inferior horn of the lateral ventricle and borders the amygdaloid nuclear complex. Although the alveus is the boundary of the amygdala and hippocampus in the sagittal plane, it is harder to detect in the infant than in the adult. The boundary of the regions can sometimes be relatively easily detected in the axial plane (Supplementary Fig. S1), especially the more medial structures, and the reference lines in the axial, as well as the sagittal plane (Supplementary Fig. S2), can be used as a guide to draw the border between the 2 in the coronal plane. In addition, it is often difficult to define the lateral margin of the amygdala in the coronal plane. However, the

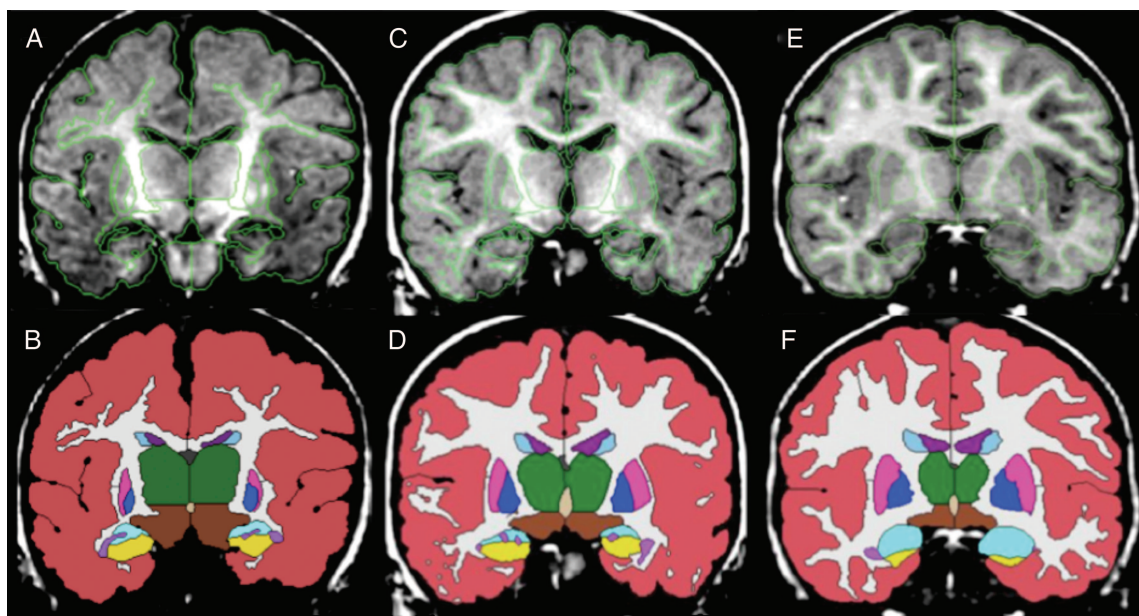


**Figure 1.** Above:  $T_1$ -weighted MRI showing segmentation of the cortical and subcortical brain regions using a thin green line in *CardViews* at (A) 3 months, (C) 6 months, (E) 12 months. Below:  $T_1$ -weighted MRI showing color code used for identification of particular structures at (B) 3 months, (D) 6 months, (F) 12 months: Thalamus (green), deep central gray (brown), putamen (pink), globus pallidum (blue), amygdala (sky blue), hippocampi (yellow), ventricular CSF (purple), white matter (white), and cerebral gray matter (red). Note: Automatically segmented cortical volume (red) and white matter volume (white) are not accurate and not used in the current analysis. At this point, manual segmentation is required to separate cortex, myelinated and unmyelinated white matter which is beyond the scope of the current paper.

- amygdala can be seen in the axial view anterior to the inferior lateral ventricle. The amygdala has lower intensity than the adjacent white matter tissue, which allows the lateral border of the amygdala to be detected. Drawing reference lines in the axial view (Supplementary Fig. S1) helps to detect the lateral margin of the amygdala in the coronal view. In the adult brain, the inferior border between the hippocampus and entorhinal cortex, as well as the posterior parahippocampal gyrus, is demarcated by white matter beneath the subiculum. In the partially myelinated infant brain, drawing the inferior border of the hippocampus in the sagittal plane helps to define the inferior border of the hippocampus (Supplementary Fig. S2), which is sometimes not clear in the coronal plane. The posterior part of the hippocampus borders the thalamus. Drawing a reference line in the sagittal view is helpful in distinguishing this transition (Supplementary Fig. S2). Drawing the posterior border of the thalamus demonstrates its posterior limits in the coronal view (Supplementary Fig. S3).
- (b) Basal ganglia. It is difficult to define the inferior border of the lenticular nucleus in the infant brain, especially in the anterior portion. One good landmark is a small horizontal portion of the medial and lateral lenticulostriate arteries that run along the inferior margin of the putamen and globus pallidus, best seen in the sagittal view. The reference line is drawn in the sagittal view along the inferior border of the lenticular nucleus (Supplementary Fig. S2). Referring to the lenticulostriate artery can guide the operator to distinguish the less well-defined inferior border of the lenticular nucleus in younger infants. The medial border of the putamen and globus pallidus is not clear because the internal capsule is not fully myelinated in the infant brain. It is recommended that the operator draw reference lines in the axial view along the medial and lateral margins of these regions (Supplementary Fig. S4) so that the volume will not be overestimated in the coronal view (Supplementary Fig. S5).
- (c) White matter. Automatic segmentation of cortical and white matter volume is not accurate using this technique and thus is not used in the current analysis. At this point, manual segmentation is required to separate cortex and white matter. Separating myelinated and unmyelinated white matter is beyond the scope of this paper. Analysis of the white matter is not included in the present study, due to time and imaging constraints.

### Volumetric Analysis

As in the technique used for the mature brain, the number of voxels in each unit on the coronal image was multiplied by the volume per voxel. The volume obtained for each unit is summated for all slices in which each unit appears (Kennedy and Nelson, 1987; Kennedy and Filipek 1989). Left- and right-sided volumes were calculated independently and added together to give the total volume. The total volume of segmented regions was then plotted.

### Statistical Analysis

(a) Volumetric growth with age and gender dimorphism. Regression analysis was performed to assess the relationship between the brain volumes and age. Although most growth data is not linear within the age range (3 to 13 months) of subjects in this study, brain growth can generally be modeled as a linear function of age (with a few exceptions). For each region we considered 2 measures of volume. The first measure was the “absolute volume” of the region; the second measure was a “normalized volume” with the whole brain as the normalizing factor, where the whole brain volume equals in the total cerebrum, total cerebellum, and brain stem without the ventricular system (Filipek et al. 1994; Caviness, Kennedy, Richelme, et al. 1996). For each region and each measure, we fit a regression model with age and gender predictors. Allowing for an interaction between age and gender and a log term for age, we choose the model that retains the important predictors while discarding extraneous terms that artificially decrease the precision of our estimates. Model selection was based on likelihood ratio tests and Akaike’s Information Criteria

(AIC). Separate models were fit for each brain region/volume measure combination.

- (b) Intra-rater reliability. In this study, 1 operator segmented 20 brain regions twice in 6 brains from each age group (i.e. 3, 4, 6, 7, 12, and 13 months) and checked the intra-rater reliability. The operator was blind to the concordance of cases across repetitions. We calculated the percent overlap of voxels (PCVs) in the 2 volume measurements (PCV). A computer program, XVOI, was utilized to determine the volumes of all analytic units. On a given coronal image, the number of voxels in each unit was multiplied by the volume per voxel. The volume obtained for each unit was summated for all slices in which each unit appears. Error checking routines were included, as were calculations to allow the determination of intra-rater reliability. For adult protocols, more than 80% of the overlap between the outcomes is considered extremely reliable. In all brain regions, except for nucleus accumbens (66.7%), the percent overlap exceeded 80% with an average percent overlap of 90.5%; 90.2% in 3 to 4 month, 88.6% in 6 to 7 month, and 92.6% in 12 to 13 month age group.
- (c) Symmetry coefficient. The symmetry coefficient (SC) was obtained for all regions of the cerebrum by each age group (i.e. 3 to 4, 6 to 7, 12 to 13 months) and for all ages combined. Comparisons between the volumes of corresponding regions of the left (L) and right (R) brain are expressed as an SC (Galaburda et al. 1987):  $SC = (L - R)/0.5(L + R)$ . Values of this index can, in principle, range from 0.0 (identical volumes in left and right) to  $\pm 2.0$  (structure present on one side only). Positive values of the index correspond to left-sided preponderance, whereas negative values of the index correspond to right-sided preponderance. Within a range of asymmetry of  $-10\%$ , a difference in value of the index of 0.01 will correspond to a 1% volumetric difference with respect to the average volume of the respective region in the 2 sides (Caviness, Kennedy, Richelme, et al. 1996). A Type 2 *t*-test was performed between the SC for the left and right “absolute volume” of all sub-regions of the cerebrum and cerebellar hemisphere.

## Results

### Volumetric Growth

Over 3 to 13 months of age, the mean absolute volume of the whole brain increased from  $645.25$  (SD  $54.66$ ) to  $970.70 \text{ cm}^3$  (SD  $75.86$ ) with  $\Delta 325.45 \text{ cm}^3$  of net volumetric increase (Supplementary Table S1). At 1 year of age, the cerebrum, exclusive of the lateral ventricles, accounts for 88.5% ( $859.28 \text{ cm}^3$ ), the cerebellum 10.4% ( $100.69 \text{ cm}^3$ ), the brainstem 1.1% ( $10.73 \text{ cm}^3$ ), and the ventricular system 0.9% ( $9.22 \text{ cm}^3$ ) of the whole brain volume. The absolute volume of the collective cerebral deep gray matter regions were  $41.81 \text{ cm}^3$  in total and this represents 4.3% of the whole brain; caudate 0.58% ( $5.61 \text{ cm}^3$ ), putamen 0.75% ( $7.29 \text{ cm}^3$ ), globus pallidum 0.28% ( $2.75 \text{ cm}^3$ ), hippocampus 0.47% ( $4.59 \text{ cm}^3$ ), amygdala 0.25% ( $2.47 \text{ cm}^3$ ), ventral diencephalon 0.68% ( $6.55 \text{ cm}^3$ ), and thalamus 1.29% ( $12.55 \text{ cm}^3$ ), and all contribute 4.9% of the cerebrum (Supplementary Table S1 and S2). Three-dimensional surface rendered images of the semi-automatically and manually segmented cerebrum and cerebellum in a sample subject at 3 and 12 months (Fig. 2) and sub-regions in a sample subject at 3, 6, and 12 months (Fig. 3) are shown.

### Volumetric Change across Time

- (a) Absolute volume. The growth trajectory of the absolute volume of the whole brain and specific regions of the brain are displayed in Supplementary Table S3 and Figures 4–8, grouped by the regions that show similar growth tendency. To summarize the results, there were 6

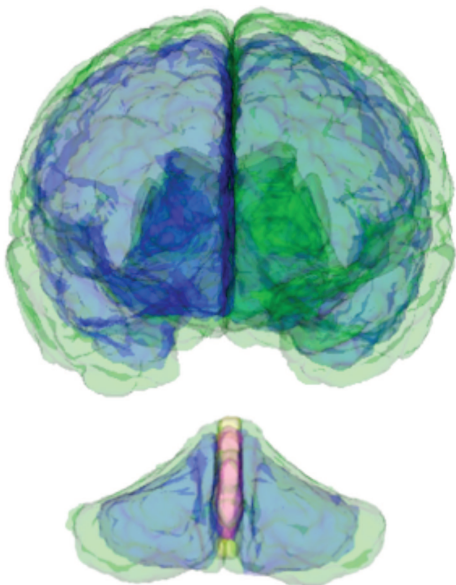


**Figure 2.** Overlapped 3D surface-rendered images of the semi-automatically segmented cerebrum (top) and cerebellum (below) in a sample subject at 3 and 12 months of age are shown for comparison. Blue, 3 months; green, 12 months; red, vermis of 3 months; yellow, vermis of 12 months.

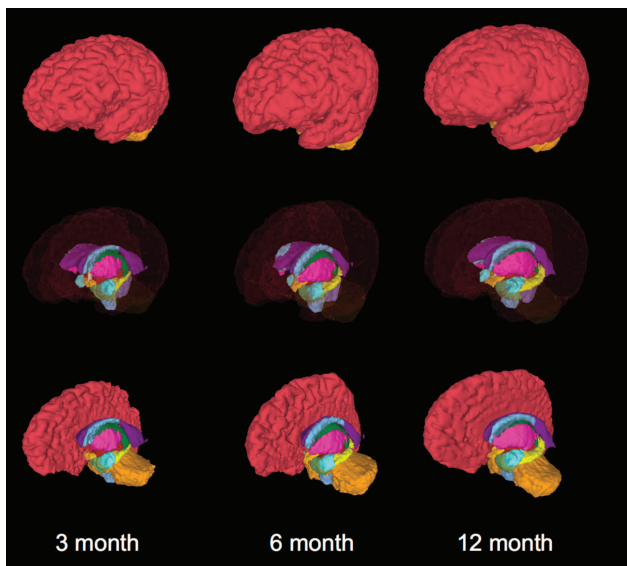


**Figure 3.** Three-dimensional surface-rendered images of the semi-automatically and manually segmented brain regions in a sample subject at 3, 6, and 12 months. Top row shows left oblique view of all brain volumes combined. Bottom row shows sub-regions after the removal of the left hemisphere. Middle row shows sub-regions in color with transparent cerebral and cerebellar hemispheres. Red, cerebral hemisphere; blue, caudate; purple, lateral ventricle; green, thalamus; pink, putamen; light blue, amygdala; yellow, hippocampus, cayenne, ventral diencephalon; orange, optic chiasm; tangerine, cerebellar hemisphere; light purple, vermis; cyan, fourth ventricle; light green, pons; blue-gray, medulla. For supplemental online 3D surface rendered images see <http://babymri.org/myong-sun.choe/>.

patterns of growth identified: (1) Figure 4a shows the pattern of no growth without gender difference (midbrain); (2) Figure 4b shows no growth with gender difference (lateral ventricles); (3) Figure 5 shows 4 regions that showed linear growth without gender difference

(hippocampus, cerebellar hemisphere, vermis, and medulla); (4) Figure 6 shows 2 regions with linear growth pattern with gender difference (thalamus and brainstem); (5) Figure 7 shows 4 regions with a logarithmic growth trajectory without any gender differences (caudate, putamen, globus pallidus, and cerebellum); and (6) Figure 8 shows 5 regions with a logarithmic growth with gender differences (whole brain, cerebrum, amygdala, ventral diencephalon, and pons). The regions were larger for male than for female in all cases when there was a sexual dimorphism.

- (b) Normalized volume. Supplementary Table S4 and Figures 9–13 show the growth trajectories for normalized volume. There were 5 patterns of growth: (1) no growth without gender differences (amygdala and medulla) (Fig. 9); (2) no growth with gender differences (caudate and vermis) (Fig. 10); (3) linear decrease without a gender effect (globus pallidus, ventral diencephalon, hippocampus, midbrain, and pons) (Fig. 11); (4) logarithmic growth without a gender effect (putamen, cerebellum, and cerebellar hemisphere) (Fig. 12); and (5) logarithmic decrease without gender differences (cerebrum, thalamus, and brainstem) (Fig. 13).

#### Absolute Volume Relative to Older Children

Caviness, Kennedy, Richelme, et al. (1996) conducted a brain volumetric study in normally developing children at 7 to 11 years of age, under a protocol that is consistent in all parameters with the present study. Both studies used  $T_1$ -weighted 3D MRI and *CardViews* to segment and analyze brain volume following the same conventions. Supplementary Table S5 shows the growth patterns of the specific regions of the brain relative to 7 to 11 years of age, which represents 95% of the volume of the adult brain (Caviness, Kennedy, Richelme, et al. 1996). The present results show that by 12 months of age some regions attain about 70% of the volume of the 7- to 11-year group (cerebrum, putamen, globus pallidus, and cerebellar hemisphere), whereas other regions develop at a slower rate attaining about 50% of the volume of the 7- to 11-year group (hippocampus and amygdala). The putamen showed the greatest volume change ( $\Delta 43.3\%$ ) from 3 to 12 months, followed by the cerebellar hemispheres ( $\Delta 33.7\%$ ) and cerebrum ( $\Delta 31.1\%$ ).

#### Gender Dimorphism

Table 2 depicts gender dimorphism for growth models in absolute volume and normalized volume. In absolute volume, male larger than female gender differences were detected in the lateral ventricles, thalamus, brainstem, whole brain, cerebrum, amygdala, ventral diencephalon, and pons. The gender differences seen in the absolute volume curves were largely absent in the normalized volume with 2 exceptions. Gender differences did exist in the trajectory curves for the “normalized” caudate and cerebellar vermis, where these regions were larger for females than males, opposite to the patterns seen in the absolute volume.

#### Symmetry Coefficient

The magnitude of laterality in each region for each age group and for all ages combined is shown in Table 3. On average,

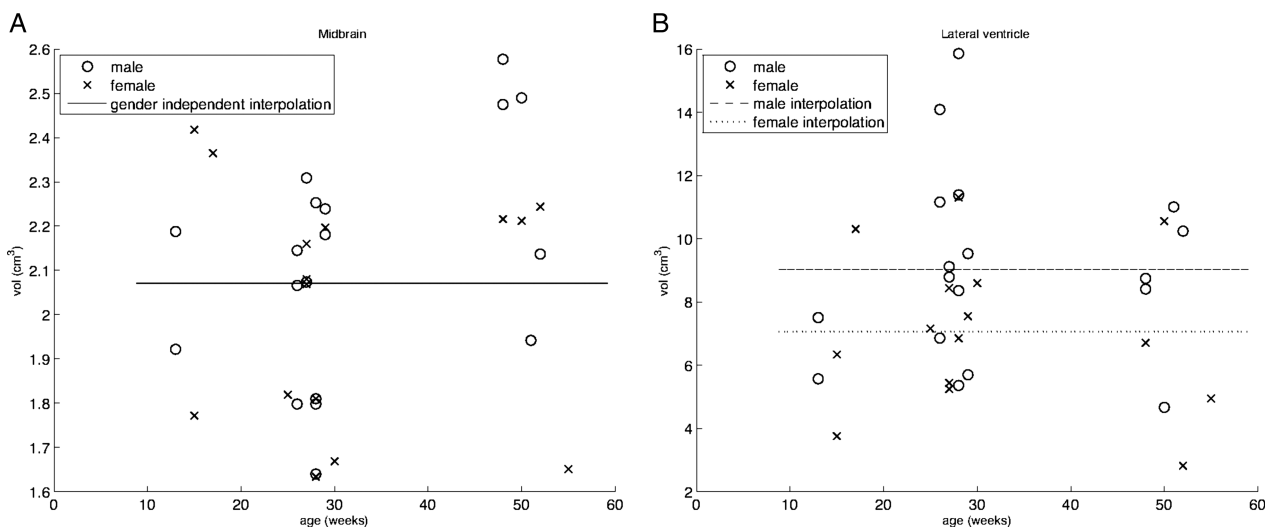


**Figure 4.** Scatter plot and regression analysis for absolute volume of 2 structures showing no growth with age. (A) Midbrain. No gender effect. (B) Lateral ventricle with a gender effect. Thirty-three brain scans. Fourteen boys and 11 girls. Five children were successfully scanned at both 6 and 12 months.

significant leftward asymmetry was observed in the cerebrum, globus pallidus, lateral ventricle, and cerebellar hemisphere ( $P=0.000$ ,  $0.000$ ,  $0.005$ , and  $0.000$ , respectively) compared with rightward asymmetry in the caudate, hippocampus, and ventral diencephalon ( $P=0.005$ ,  $0.000$ , and  $0.000$ , respectively) for all ages combined. In the 3- to 4-month age group, thalamus and putamen were larger on the left than on the right ( $P=0.005$  and  $0.009$ , respectively). In the 6- to 7-month age group, cerebrum, globus pallidus, lateral ventricle, and cerebellar hemisphere ( $P=.009$ ,  $0.000$ ,  $0.046$ , and  $0.000$ , respectively) were larger on the left than on the right, while caudate, hippocampus, and ventral diencephalon ( $P=0.03$ ,  $0.049$ , and  $0.002$ , respectively) were larger on the right when compared with the left side. Leftward asymmetry was observed in the globus pallidus ( $P=0.000$ ) and rightward asymmetry in the putamen, hippocampus, and ventral diencephalon ( $P=0.04$ ,  $0.02$ , and  $0.02$ , respectively) in the 12- to 13-month age group. Only the putamen showed a significant switch in symmetry from left ( $P=0.009$ ) at 3 to 4 months to right ( $P=0.04$ ) at 12 to 13 months (Supplementary Figure S8).

## Discussion

Although the overall high rate of postnatal brain growth that occurs during the first year of life has been reported (Knickmeyer et al. 2008; Gilmore et al. 2011; Shi et al. 2011) differential growth patterns of “sub-regions” have remained largely unknown and unexplored. Applying a detailed, neuroanatomical, knowledge-based, semi-automated brain segmentation and analysis system to infant brain, we are beginning to unravel longstanding questions about heterochronic growth patterns of global and regional brain volumes in the first postnatal year, which is a critical period of human brain development. We present here absolute and normalized volumes of the brain and sub-regions in incompletely myelinated developing infant brains. Furthermore, we have fitted growth models for each brain region and characterized 6 different growth patterns for absolute volume and 5 patterns for

normalized volume. It is important to note that we were able to accomplish challenging and demanding brain segmentation within typically developing infant brain, achieving high intra-rater reliabilities. Although previous volumetric studies at early ages have provided us invaluable information about early brain development (Matsuzawa et al. 2001; Nishida et al. 2006; Gilmore et al. 2007; Knickmeyer et al. 2008), to our knowledge, this is the first study that provides detailed information on regional brain growth between 3 and 13 months.

## Regional Heterochronicity

Several distinct growth patterns with differential growth rates were observed in the brain regions analyzed in this study. If growth was detected, it was determined whether the growth was linear or logarithmic. These types of growth were chosen as they fit with the expectation that the regional growth should be self-limited and therefore fit a Gompertz function (Gompertz 1825; Gilles et al. 1983). Therefore, in the rapid growth phase, a linear fit would be appropriate whereas when growth begins to slow, a logarithmic fit would be most appropriate as seen for the Gompertz function.

In the absolute volume, all the brain regions, except for the midbrain, showed a significant growth from 3 to 13 months (12 to 55 weeks). This was particularly evident for the absolute volume of the putamen, cerebellar hemisphere, cerebellum, and fourth ventricle, where we defined a near 2-fold increase (1.98, 1.78, 1.75, and 1.72, respectively) from 3 to 13 months (Supplementary Table S1). When the volume is normalized, the accelerated growth rate of the putamen, cerebellar hemisphere, and total cerebellum were observed (Supplementary Table S2), suggesting that the volumetric growth rate of these regions was greater than that of the whole brain volume during this period. On the other hand, the growth rate relative to the whole brain volume decreased over time with a linear age model being the best fit for the globus pallidus, ventral diencephalon, hippocampus, midbrain, and pons, and with a logarithmic age model being the best fit for the cerebrum, thalamus, and

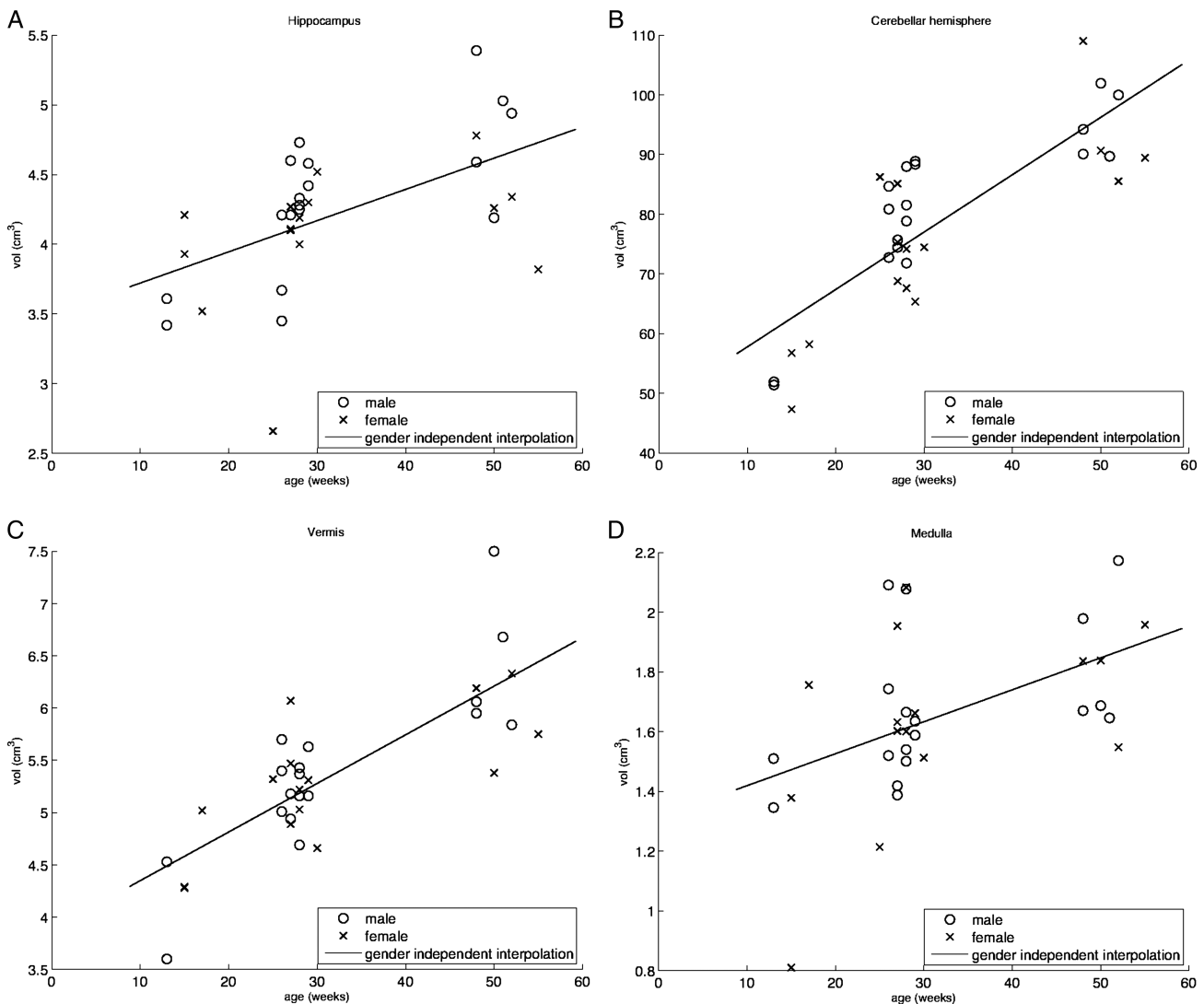


**Figure 5.** Scatter plot and regression analysis for absolute volume of 4 regions with a linear growth pattern without gender effects. (A) Hippocampus, (B) cerebellar hemisphere, (C) vermis, and (D) medulla.

brainstem. As a whole, putamen, cerebellar hemisphere, and total cerebellum were the only regions that showed an accelerated growth as a percentage of the whole brain volume in this phase.

The fastest growing regions are thought to be most metabolically active. If we assume that the brain regions undergoing most rapid growth are most vulnerable to the negative effects of endogenous and exogenous insults (Huppi et al. 1998; Volpe 2009), then the putamen, cerebellar hemispheres, and cerebellum as a whole are, based on our data, particularly vulnerable in infancy because of their significant rapid growth. Knickmeyer et al. (2008) has reported striking increases of cerebellar absolute volume as well as a disproportionate enlargement in the normalized brain by total brain volume during the first year of life. Traditionally, the cerebellum has been thought to be primarily involved in motor-related functions, including coordination of movements and balance. However, studies using physiological and behavioral measures have also implicated the

cerebellum in the regulation of cognitive and emotional processing (Schmahmann et al. 2007). The putamen is part of the basal ganglia circuit loop that plays an important role in learning (Packard and Knowlton 2002) and in the motor skills, particularly in initiation and execution of somatic motor activity subserving control of voluntary movement. Histologically, a rapid increase of vessel density in the putamen after birth has been observed (Miyawaki et al. 1998; Takashima et al. 2009) and this vessel development could explain the rapid volumetric growth in the putamen found in this study. Significant relationships between general cognitive ability (IQ) and the volume of sub-cortical brain regions (cerebellum and caudate) as well as executive function (spatial working memory) and the putamen in school children (6 to 13 years) were found in Pangalinan et al.'s study (2010). The results detailed here can begin to explain even earlier relationships between brain volumes and the development of both cognitive and motor abilities across the first year of life.

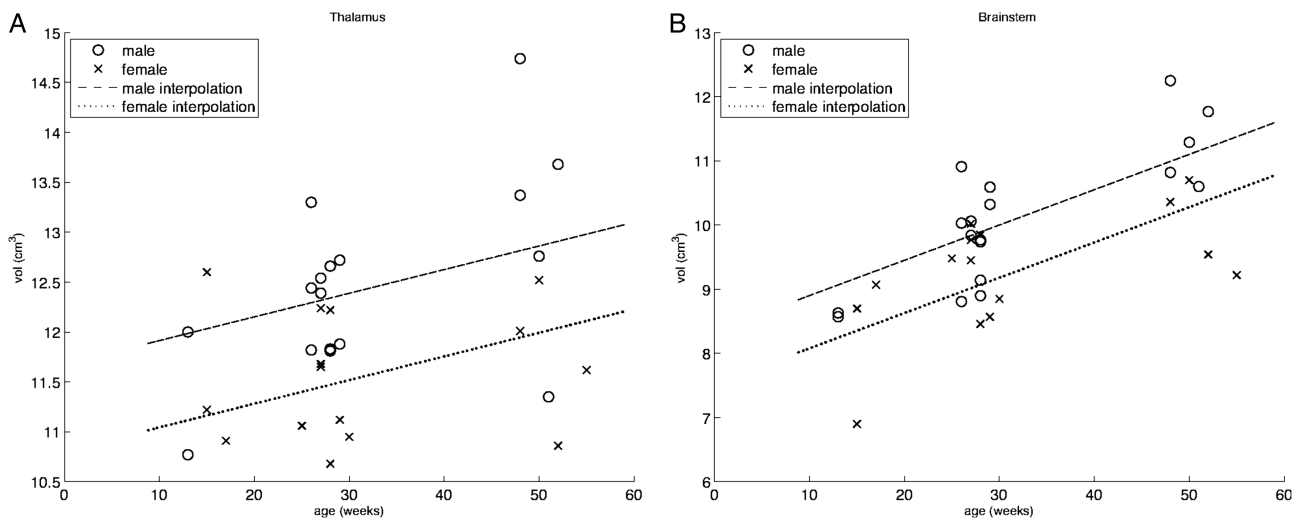


**Figure 6.** Scatter plot and regression analysis for absolute volume of 4 regions with a linear growth pattern with a gender effect. (A) Thalamus and (B) brainstem.

Our results show relatively slower growth in amygdala and hippocampus during infancy before reaching its expected full volume (46.5% and 56.1% of 7 to 11 year olds, respectively) (Supplementary Table S5). The volume of the anterior temporal lobes increases sharply until the age of 2 years (Utsunomiya et al. 1999), and active maturation of the amygdalae and hippocampal volumes is also expected to continue after the first year. Associations between amygdala size and language outcomes have been reported in adults (Haznedar et al. 2000) and children with autism (Munson et al. 2006; Cauda et al. 2011; Rudie et al. 2012). Our recent report (Ortiz-Mantilla et al. 2010) extended this association to normally developing children, supporting the idea that the amygdalae might play an important but as yet unspecified role in mediating language acquisition. These findings may yield useful information about the patterns of typical versus atypical development, thus facilitating early intervention decisions designed to improve outcomes in children diagnosed as autistic.

Importantly, these results as a whole will contribute to our progressive understanding of the diverse underpinnings of neurological diseases in infancy. In particular, differential growth rates may well be sensitive indices of disease processes where differing principles of pathogenesis and progression may be expected to express correspondingly differential patterns of growth aberration. Thus the pattern expressed in a systems' degeneration such as progyria will differ from that biased to a tissue compartment such as leukodystrophy. Infection, on the other hand, may have little or no anatomic systems' bias. General perfusion collapse will target border zones or regions of high metabolic demand while specific vessel occlusion might well be expressed in the respective perfusion territory. However, in all these cases, a better understanding of the scope of differential growth patterns over typical development will allow more informed analysis of pathological divergence.

#### Gender Dimorphism

Once normalized to the whole brain volume, few gender-specific volumetric differences remained. However, gender differences did persist particularly in caudate and vermis.

Normalized caudate and cerebellar vermis volumes were smaller in males than in females across age and remained constant in proportion to whole brain volume. Interestingly, smaller caudate volumes have been reported in patients with ADHD (Castellanos et al. 2002), suggesting that the consistently smaller caudate in males might contribute to their higher vulnerability to ADHD (males:females = 3:1) (Szatmari et al. 1989). Smaller cerebellar vermal volumes when compared with normally developing children have been reported in autism spectrum disorder (ASD) studies as well (Courchesne et al. 1988, 1994, 2001; Ciesielski et al. 1997; Levitt et al. 1999; Kaufmann et al. 2003; Webb et al. 2009) which might help to explain the 4 times higher prevalence in males than in females in ASD (Kriegman et al. 2007).

#### Asymmetry

Cerebral asymmetry has been suggested to be a developmental event, mostly genetically mediated by evolutionary and molecular mechanisms, and present as early as 20 weeks of gestation (Sun and Walsh 2006; Kasprian et al. 2011). In line with reports in neonates (Gilmore et al. 2007), and opposite to the pattern shown by older children and adults (Giedd, Snell, et al. 1996; Sowell and Jernigan 1998; Nopoulos et al. 2000; Good et al. 2001; Matsuzawa et al. 2001; Toga and Thompson 2003; Raz et al. 2004), we found a leftward cerebral asymmetry across the first year of life. Our analysis suggest that the hemispheric shift in laterality from larger left to larger right cerebrum occurs after the first year of life as a result of the maturation process that likely reflects genetic programming and effects of experience (Gilmore et al. 2007). The later rightward asymmetry found in older children and adults may be related to differences in growth and myelination with the frontal lobes maturing later than the occipital lobes (Shaw et al. 2008).

Similar to that reported in young adults (Szabó et al. 2003; Diedrichsen et al. 2009), but in contrast to reports in children and adolescents (Giedd, Snell, et al. 1996), we found the left cerebellar hemisphere larger than the right. As structural asymmetry appears to underlie functional asymmetry (Toga and Thompson 2003), the cerebellar asymmetry observed

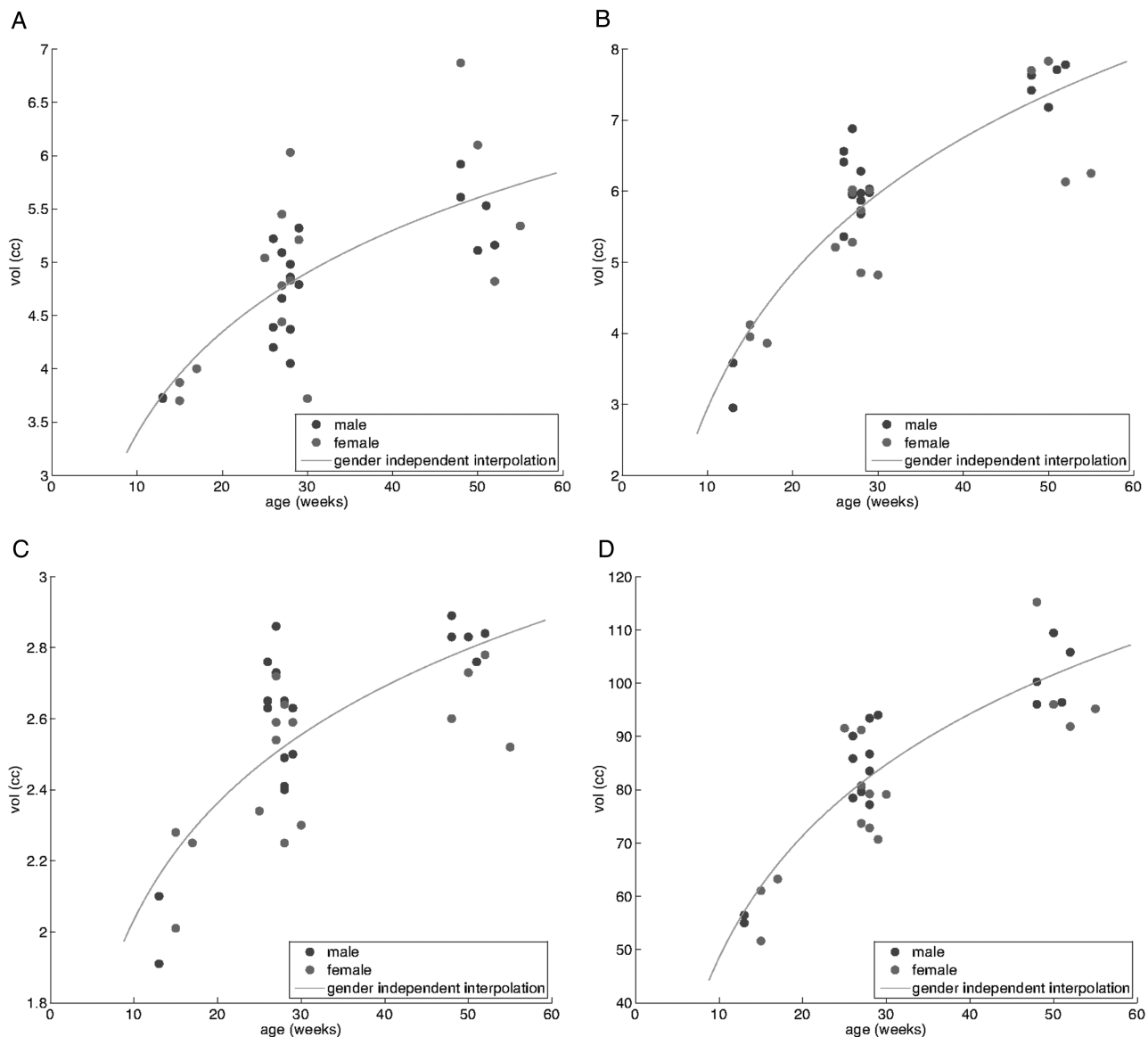


**Figure 7.** Scatter plot and regression analysis for absolute volume of 4 regions with a logarithmic growth pattern without gender effects. (A) Caudate, (B) putamen, (C) globus pallidus and (D) cerebellum.

during the first year of life may represent a transitory maturation step in a period characterized by the increasing development of motor coordination and balance. A meta-analytic study found evidence for functional cerebellar asymmetry; language/verbal working memory processes were right lateralized while spatial and motor learning processing showed larger left cerebellar activation (Hu et al. 2008; Stoodley and Schmahmann 2009). As is the case later in development when language abilities and executive functions emerge, more involvement of the right cerebellar hemisphere might be expected after the first year, thus decreasing the degree of cerebellar asymmetry observed during infancy.

Asymmetric developmental trajectories were also found in the basal ganglia, a group of nuclei involved in motor regulation and learning (Packard and Knowlton 2002). Similar to prior reports in older children (Giedd, Snell, et al. 1996; Reiss et al. 1996), we found larger right caudates when all ages were combined. However, in adults, the results published to

date are somewhat inconsistent. Recently, volumetric asymmetry for caudate favoring the right side (Ifthikharuddin et al. 2000; Watkins et al. 2001; Looi et al. 2008; Madsen et al. 2010; Yamashita et al. 2011) has been reported, although earlier studies found larger left side (Gunning-Dixon et al. 1998) or even no asymmetry (Sowell and Jernigan 1998). Our findings suggest that the right-lateralized pattern of caudate growth is already present in infancy and may not change significantly across age.

One puzzling finding was the change in asymmetry of the putamen across the first year. While leftward asymmetry was seen at 3 to 4 months, no difference in laterality was found at 6 to 7 months. However, by 12 to 13 months of age, the right putamen was found to be consistently larger than the left putamen. Although we must raise the caveat of a modest sample size, particularly at the 3- to 4-month age point, these data could suggest that across the first year of life the putamen may undergo rapid dynamic changes that are

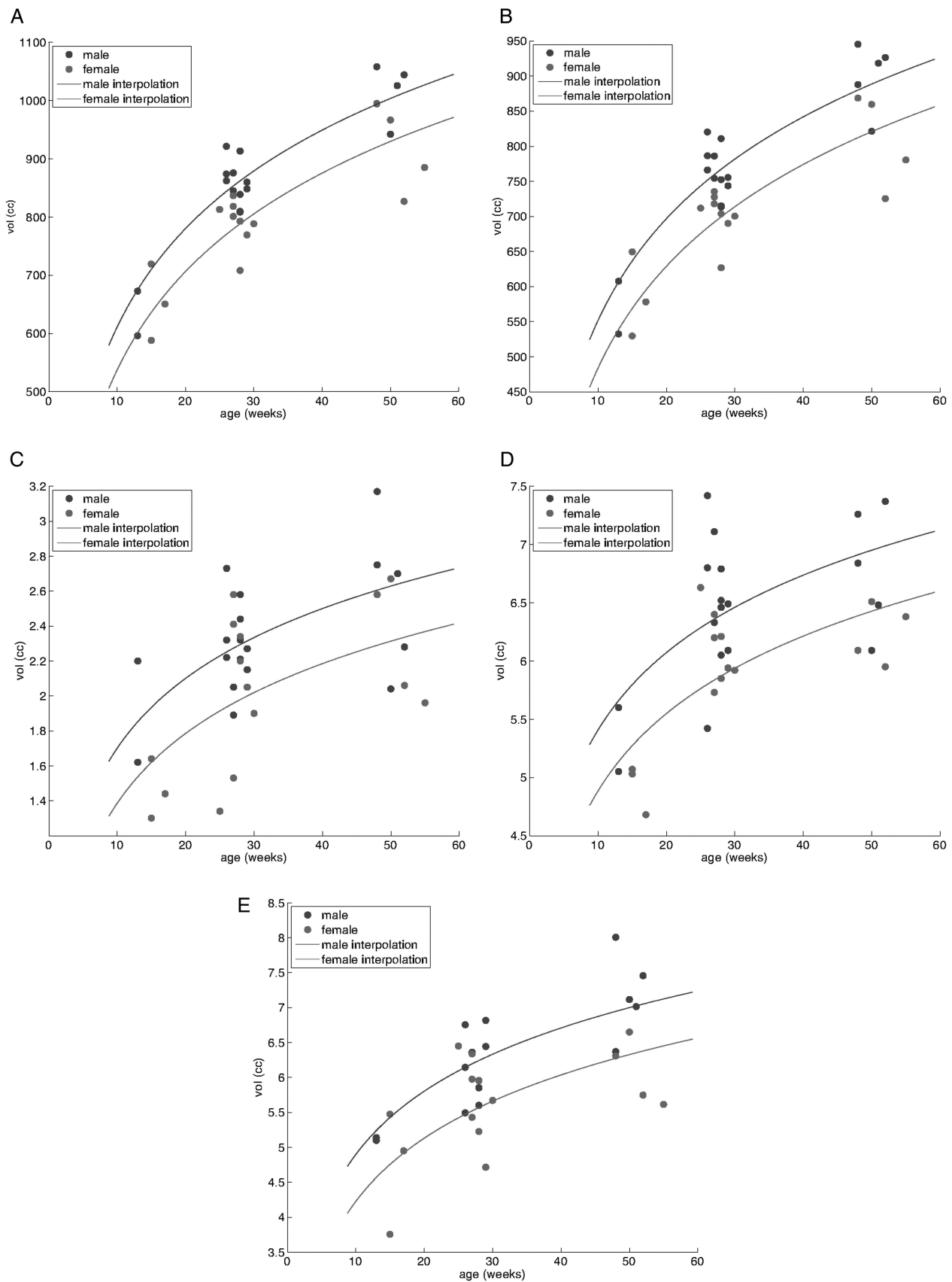


**Figure 8.** Scatter plot and regression analysis for absolute volume of 5 regions with a logarithmic growth pattern with a gender effect. (A) Whole brain, (B) cerebrum, (C) amygdala, (D) ventral diencephalon, and (E) pons.

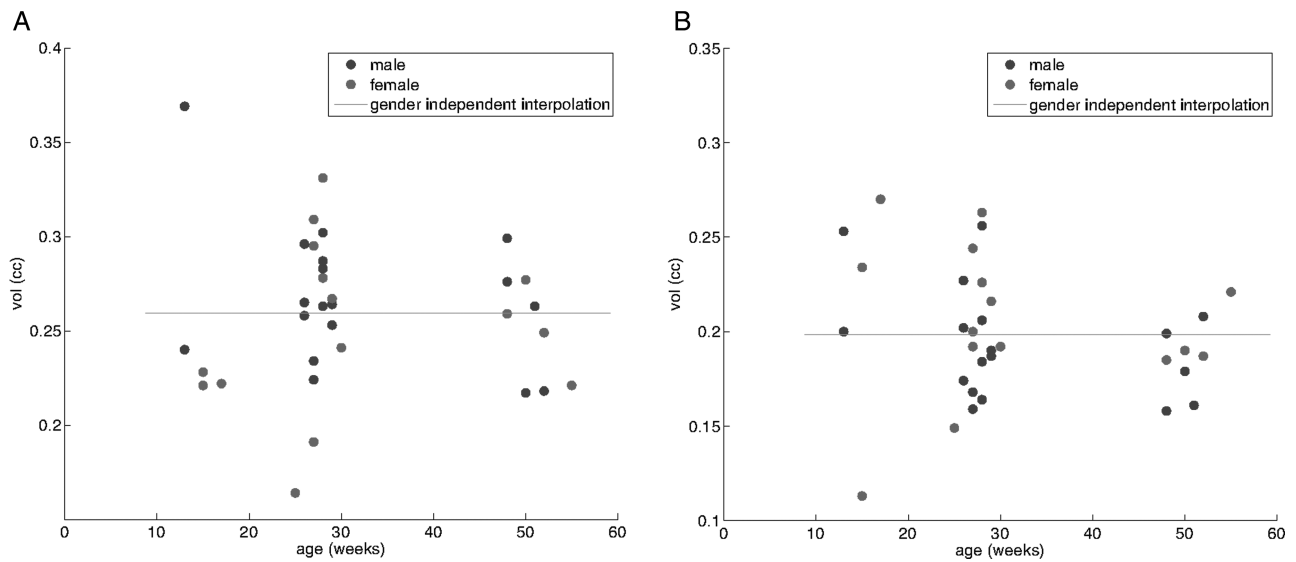


**Figure 9.** Scatter plot and regression analysis for normalized brain volumes of 2 regions with no growth pattern and gender effects. (A) Amygdala and (B) medulla.

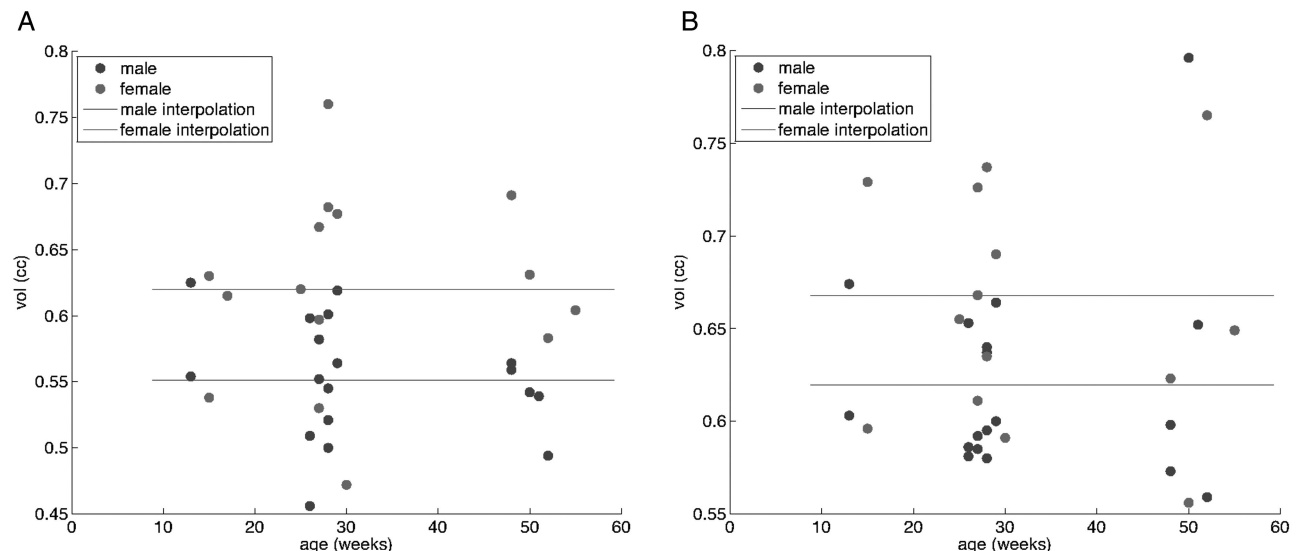


**Figure 10.** Scatter plot and regression analysis for normalized brain volumes of 2 regions with no growth pattern with gender effect. (A) Caudate and (B) vermis.

reflected in variations in laterality across age (Supplementary Fig. S3). At later ages, conflicting results are also found in the literature: Leftward asymmetry in children and adolescents (Giedd, Snell, et al. 1996; Wellington et al. 2006) and rightward asymmetry in both older children (Caviness, Kennedy, Richelme, et al. 1996) and adults (Gunning-Dixon et al. 1998). Hence, to accurately characterize the growth pattern of the putamen and to reconcile these contradictory results, longitudinal studies including additional age points and larger samples are warranted.

Our results also indicated significant volumetric asymmetry for the globus pallidus favoring the left side, alike to what has been found in older children (Caviness, Kennedy, Richelme, et al. 1996) and adults (Raz et al. 1995). Thus, the leftward laterality in the globus pallidus appears to be stable throughout life.

Rightward asymmetry in the hippocampus has been reported in pre- and full-term newborns (Thompson et al.

2009), older children, adolescents (Giedd, Vaituzis, et al. 1996; Pfluger et al. 1999), and older adults (Jack et al. 1989; Li et al. 2007; Ystad et al. 2009). Similarly, we found a consistent rightward hippocampal asymmetry in infants, suggesting that right hippocampal dominance is present at birth and persist across age. The right hippocampus is critical for episodic and spatial memory formation (Burgess et al. 2002). Stronger functional connectivity between the right hippocampus and the posterior cingulate cortex has been found to predict better performance in episodic memory tasks (Wang et al. 2010) and the right hippocampal damage, impairment in spatial memory (Bohbot et al. 1998).

#### Limitations and Future Prospects

- (a) Better images with improved technology. The MR image contrast changes rapidly across development due to axonal pruning and myelination, which is one of the

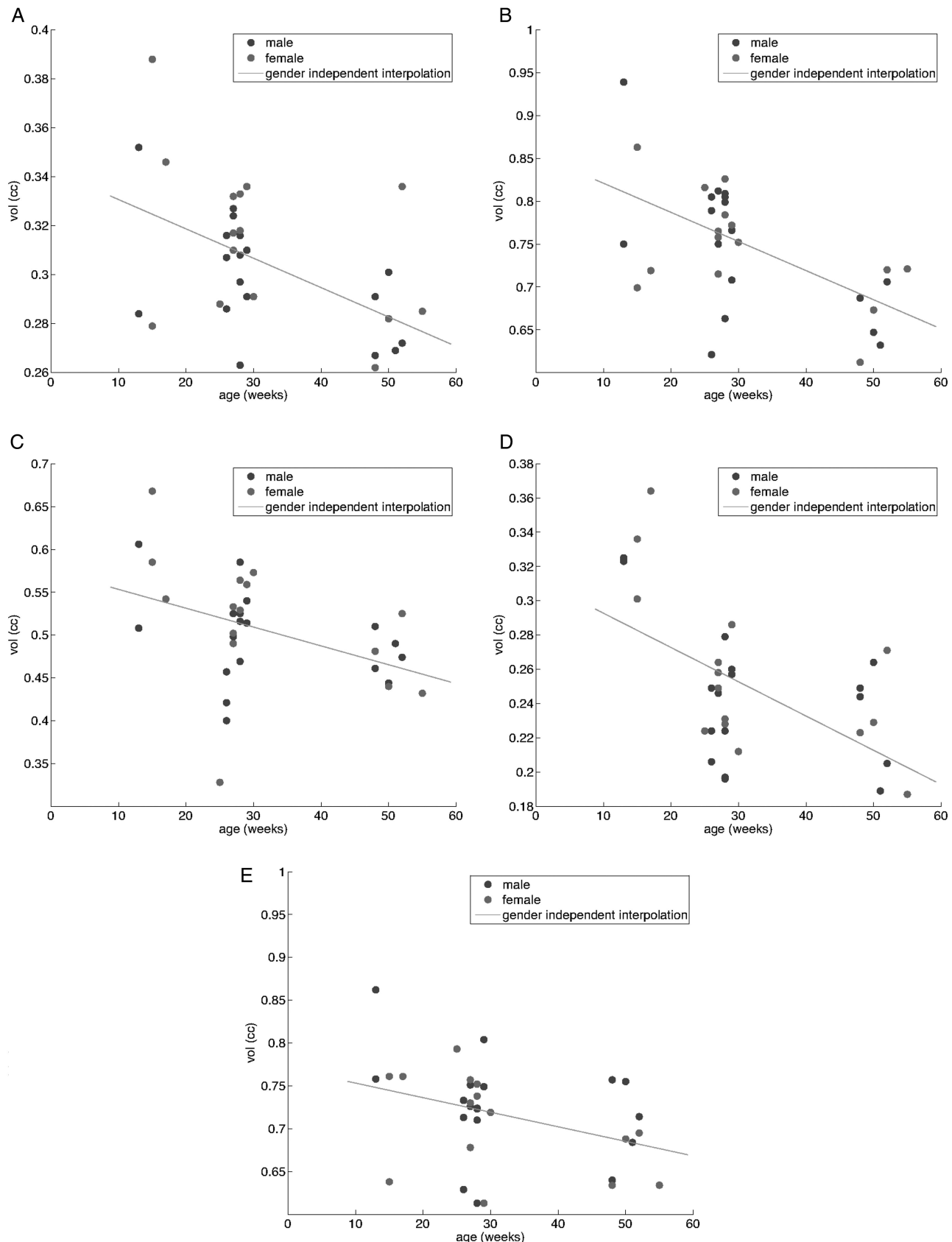


**Figure 11.** Scatter plot and regression analysis for normalized brain volumes of 5 regions with a linear decrease without gender effects. (A) Globus pallidus and (B) ventral diencephalon, (C) hippocampus, (D) midbrain, and (E) pons.

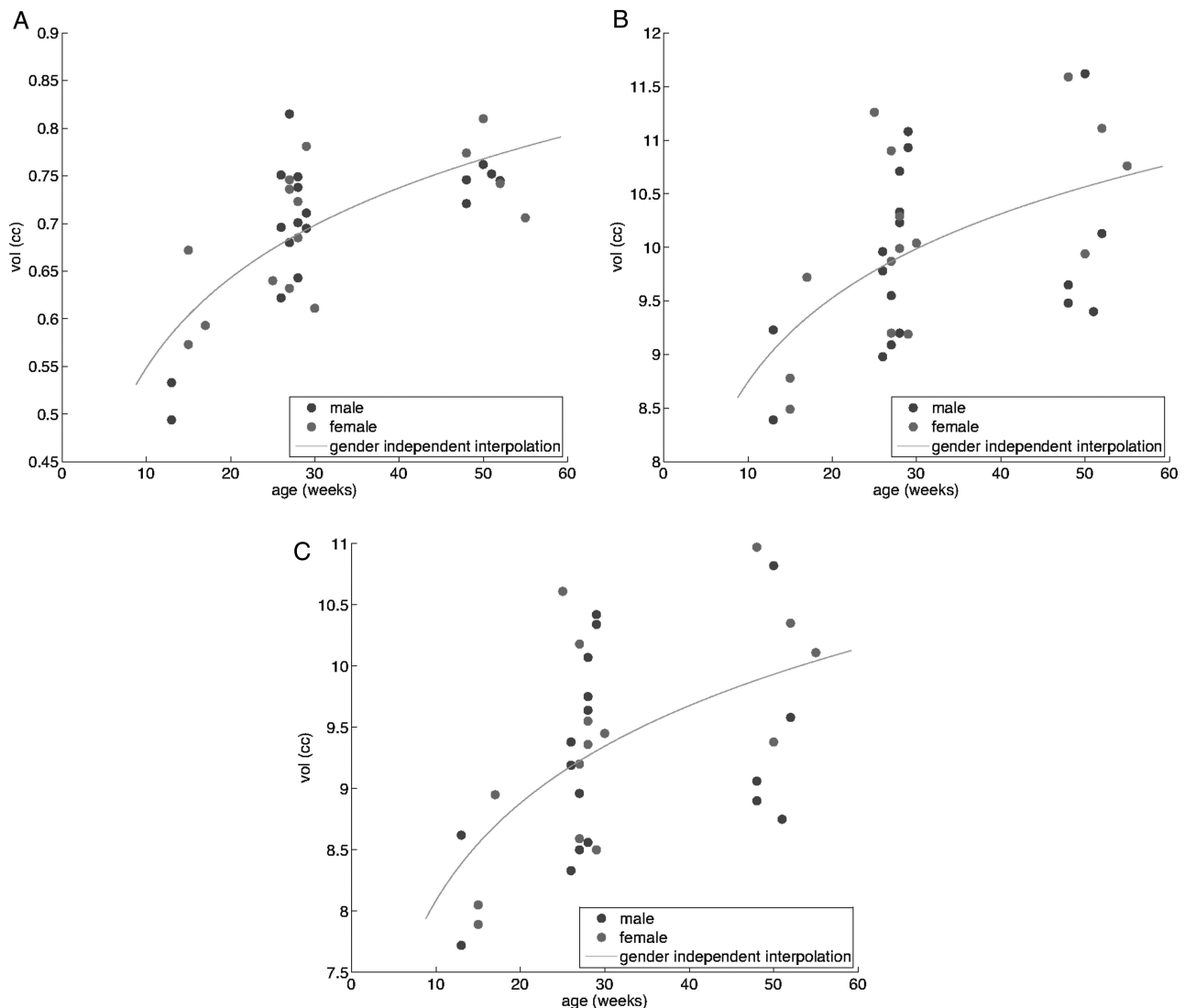


**Figure 12.** Scatter plot and regression analysis for normalized brain volumes of 3 regions with a logarithmic growth pattern without gender effects. (A) Putamen, (B) whole cerebellum, and (C) cerebellar hemisphere.

main developmental achievements in infancy. The fidelity of the distinction of gray matter versus white matter in MR images with improved technology is one of the main issues that remain to be resolved. Holland et al. (1986), McArdle et al. (1987), Bird et al. (1989), van der Knaap and Valk (1990), and Barkovich (2005) have reported stages and milestones of normal brain myelination on MRI. In order to facilitate better assessment of children at higher risk of developmental disorders, white matter volumetric measurements have been undertaken in infant, child, and adolescent brains (Paus et al. 2001; Lenroot et al. 2007; Knickmeyer et al. 2008), with some success. However, more accurate quantification techniques need to be explored. Although  $T_2$ -weighted images have been used in fetal and neonatal studies (Yu et al. 2010; Glasel et al. 2011; Kasprarian et al. 2011; Wang et al. 2011), we chose volumetric  $T_1$ -weighted images for this study that spanned the ages of 3 to 13 months. This allowed comparison to many of the prior studies in older children that have been almost exclusively performed using volumetric  $T_1$ -weighted images. Future projects will

focus on the better images that can be obtained with improved technology and will include analysis of both  $T_1$  and  $T_2$  contrasts to allow better definition of cortical gray and white matter boundaries.

- (b) Regression modeling limitations. The usual caveats for regression modeling hold for this dataset. We cannot extrapolate beyond the ages of 3 to 13 months. In addition, we had fewer subjects at the 3- and 4-month age period than for the older ages. These data points have the potential to be overly influential for the coefficient estimates and potentially for the choice of optimal model as well. An assumption of self-limiting growth was applied to all the brain regions. However, the regions that showed linear growth in our analysis could have shown a logarithmic growth pattern, if more data points were added for the 3- to 4-month age period. This would be consistent with the gradual asymptote seen for the Gompertz function.
- (c) Expand age range and number. The results for our volumetric growth trajectories may only be applied to the specific age span studied here, specifically for 3 to 13

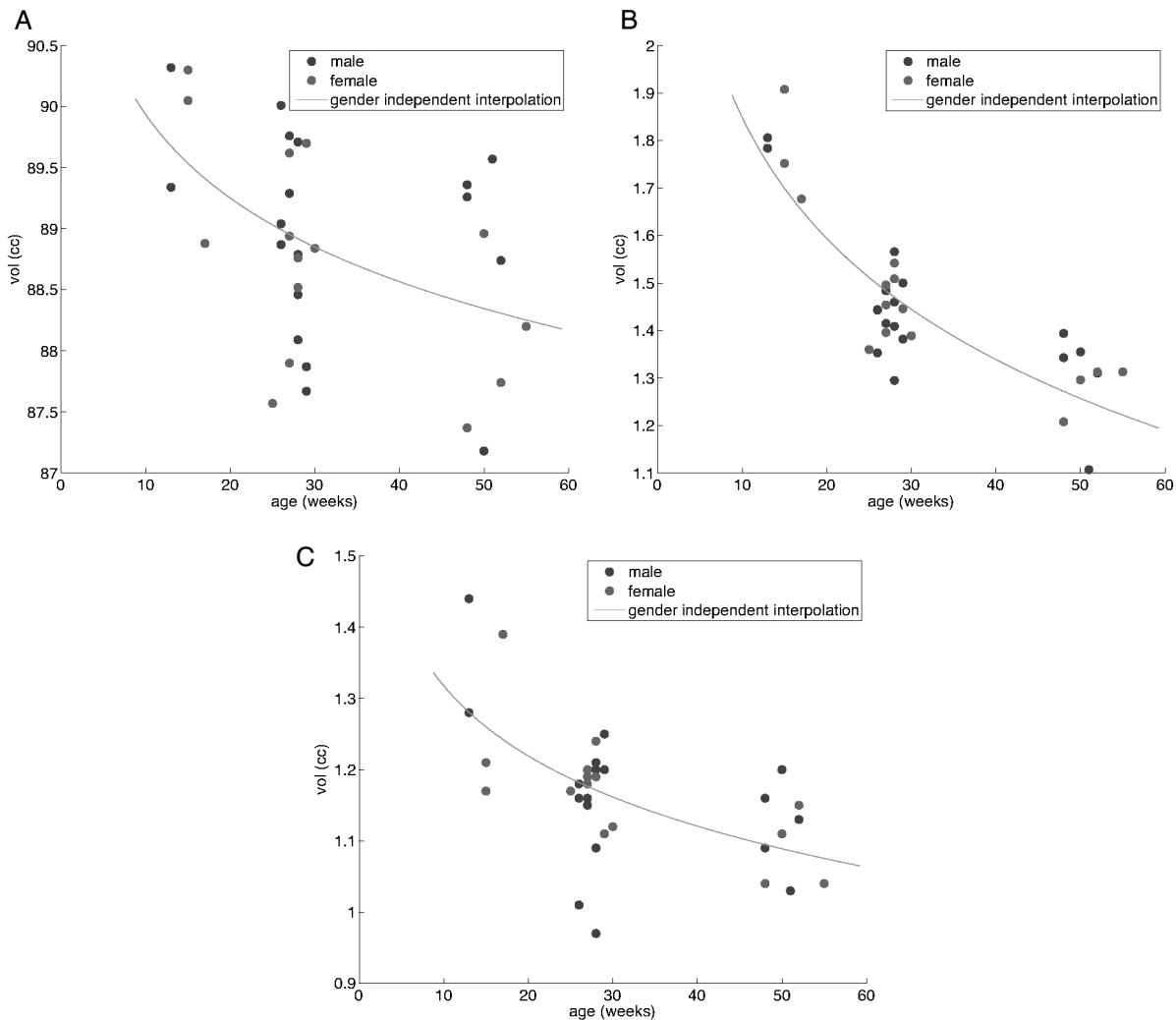


**Figure 13.** Scatter plot and regression analysis for normalized brain volumes of 3 regions with a logarithmic decrease pattern without gender effects. (A) Cerebrum, (B) thalamus, and (C) brainstem.

months. In this study, the relatively small sample size, the gender distribution in each age group, and the cross-sectional sample might have affected the projected trajectories. The growth rates of the brain and its sub-regions would have shown the most rapid brain growth across the first 3 months of life. Therefore, future studies that include fetal and neonatal periods as well as the first 3 months will be extremely important in order to better characterize regional growth trajectories in typical early brain development.

Further studies are critical and should be performed in combination with diffusion tensor imaging and tractography, to shed light on the neural mechanisms that underlie the dramatic physical, psychological, cognitive, and language development that occurs over the first year of life. We are also interested in examining how structural volume, axonal development, and myelination correlate with development in physical, psychological, cognitive, behavioral, attentional, and socialization in early human life. All children in this study have received detailed prospective neurobehavioral testing across multiple years and thus future projects will explore the

**Table 2**  
Gender dimorphism for the growth model

	Absolute volume	Normalized volume = absolute volume/WB
Male > Female	Whole brain Cerebrum Thalamus Ventral diencephalon Amygdala Lateral ventricles Brainstem Pons	
Female > male		Caudate Vermis
Male = female	Caudate Putamen Globus pallidus Hippocampus Cerebellum Cerebellar hemisphere Vermis Midbrain Medulla	Cerebrum Putamen Globus pallidus Thalamus Ventral diencephalon Amygdala Hippocampus Cerebellum Cerebellar hemisphere Brainstem Midbrain Pons Medulla

Note: WB, whole brain.

**Table 3**  
Symmetry coefficient (SC)

	3–4 months (13–17 weeks)						6–7 months (26 to 30 weeks)						12 to 13 months (48 to 55 weeks)						3 to 13 months (12 to 55 weeks)					
	R mean (SD) (cm <sup>3</sup> )	L mean (SD) (cm <sup>3</sup> )	SC	P	R mean (SD) (cm <sup>3</sup> )	L mean (SD) (cm <sup>3</sup> )	SC	P	R mean (SD) (cm <sup>3</sup> )	L mean (SD) (cm <sup>3</sup> )	SC	P	R mean (SD) (cm <sup>3</sup> )	L mean (SD) (cm <sup>3</sup> )	SC	P	R mean (SD) (cm <sup>3</sup> )	L mean (SD) (cm <sup>3</sup> )	SC	P				
Cerebrum	291.74 (26.70)	292.95 (26.51)	0.4	0.2	<b>367.51 (22.60)</b>	<b>370.21 (23.48)</b>	<b>0.7</b>	<b>0.009</b>	417.35 (35.85)	417.77 (36.69)	0.3	0.3	<b>372.59 (52.05)</b>	<b>382.83 (53.13)</b>	<b>2.7</b>	<b>0.000</b>								
Thalamus	<b>5.62 (0.37)</b>	<b>5.88 (0.42)</b>	<b>4.6</b>	<b>0.005</b>	5.98 (0.34)	5.96 (0.34)	-0.3	0.5	6.23 (0.61)	6.31 (0.65)	1.3	0.3	5.99 (0.46)	6.05 (0.47)	0.9	0.08								
Putamen	<b>1.81 (0.22)</b>	<b>1.88 (0.24)</b>	<b>4.2</b>	<b>0.009</b>	2.90 (0.26)	2.88 (0.31)	0.9	0.5	<b>3.70 (0.34)</b>	<b>3.59 (0.33)</b>	-2.8	0.4	2.95 (0.66)	2.95 (0.62)	0.4	0.7								
GP	<b>0.97 (0.12)</b>	<b>1.13 (0.10)</b>	<b>15.6</b>	<b>0.008</b>	1.22 (0.08)	<b>1.34 (0.10)</b>	<b>9.3</b>	<b>0.000</b>	<b>1.31 (0.09)</b>	<b>1.45 (0.05)</b>	<b>10.2</b>	<b>0.000</b>	<b>1.21 (0.14)</b>	<b>1.34 (0.13)</b>	<b>10.5</b>	<b>0.000</b>								
Caudate	1.92 (0.10)	1.88 (0.05)	-2.1	0.4	<b>2.43 (0.29)</b>	<b>2.38 (0.26)</b>	-1.7	0.3	2.83 (0.36)	2.78 (0.27)	-1.7	0.2	<b>2.46 (0.41)</b>	<b>2.41 (0.37)</b>	-1.8	<b>0.005</b>								
Amygdala	0.90 (0.18)	0.74 (0.22)	-21.7	0.1	<b>1.06 (0.20)</b>	<b>1.13 (0.18)</b>	<b>7.0</b>	<b>0.05</b>	1.26 (0.17)	1.20 (0.27)	-6.4	0.3	1.09 (0.22)	1.09 (0.26)	-1.0	0.8								
Hippocampus	1.94 (0.22)	1.80 (0.14)	-6.9	0.2	<b>2.11 (0.22)</b>	<b>2.04 (0.27)</b>	-3.8	0.05	<b>2.36 (0.27)</b>	<b>2.23 (0.24)</b>	-5.4	0.02	<b>2.15 (0.27)</b>	<b>2.06 (0.28)</b>	-4.7	<b>0.000</b>								
VDC	2.57 (0.17)	2.52 (0.18)	-1.9	0.3	<b>3.20 (0.26)</b>	<b>3.13 (0.23)</b>	-2.3	0.002	<b>3.33 (0.28)</b>	<b>3.22 (0.24)</b>	-3.4	0.03	<b>3.14 (0.36)</b>	<b>3.06 (0.32)</b>	-2.5	<b>0.000</b>								
LV	0.66 (0.99)	0.77 (1.33)	-1.8	0.9	<b>4.07 (1.46)</b>	<b>4.71 (1.76)</b>	<b>13.0</b>	<b>0.05</b>	3.47 (1.42)	4.10 (1.67)	14.6	0.09	<b>3.78 (1.42)</b>	<b>4.35 (1.68)</b>	14.0	<b>0.005</b>								
Cerebellar hemisphere	26.65 (2.39)	26.47 (2.04)	-0.6	0.6	<b>38.74 (3.62)</b>	<b>39.30 (3.78)</b>	<b>1.4</b>	<b>0.000</b>	47.07 (3.79)	47.43 (3.81)	0.8	0.08	<b>39.14 (7.40)</b>	<b>39.62 (7.45)</b>	1.2	<b>0.000</b>								

Note: The brain regions with significant differences in laterality ( $P < 0.05$ ) are given in bold.  
GP: globus pallidus; VDC: ventral diencephalon; LV: lateral ventricles.

predictive power of this early volumetric growth to behavioral outcomes (e.g. Ortiz-Mantilla *et al.* 2010).

In summary, we conducted volumetric analysis in typically developing infant brains (aged over 3 to 13 months) using neuroanatomical, knowledge-based, detailed semi-automated analysis techniques. We were able to construct models for normal brain growth trajectories for each region, including individual cerebral deep gray matter structures. Quantitative data, especially with larger numbers of subjects and, most importantly, continuity within the first 3 months of development when there is exponential growth of all brain regions, should result in reliable milestones for infant regional brain development. The data collected in this study represent the beginning of better understanding of the character and importance of regional brain growth trajectories.

## Supplementary Material

Supplementary material can be found at: <http://www.cercor.oxfordjournals.org/>.

## Notes

We would like to thank Professor Yoshio Okada for constructive feedback on this manuscript. We also thank D. Danielle Sliva, Kiho Im, and Emi Takahashi for editorial comments. The authors gratefully acknowledge the infants and their parents who participated in this study as well as the researchers and staff at the Center for Molecular and Behavioral Neuroscience who spent many hours patiently acquiring the used data. The authors also acknowledge the considerable efforts of the staff at The Center for Morphometric Analysis who also contributed to the study.

## Funding

This research was supported by the Thrasher Research Fund, the Santa Fe Institute Consortium, the William Randolph Hearst Fund of Harvard University, NIH K23NS042758, NIH R21EB008547 and by NSF #SBE-0542013 (to the Temporal Dynamics of Learning Center) with additional funding from the Elizabeth H. Solomon Center for Neurodevelopmental Research.

## References

- Barkovich AJ. 2005. Magnetic resonance techniques in the assessment of myelin and myelination. *J Inher Metab Dis.* 28(3): 311–343.
- Bird CR, Hedberg M, Drayer BP, Keller PJ, Flom RA, Hodak JA. 1989. MR assessment of myelination in infants and children: Usefulness of marker sites. *AJNR Am J Neuroradiol.* 10(4):731–740.
- Bohbot VD, Kalina M, Stepankova K, Spackova N, Petrides M, Nadel L. 1998. Spatial memory deficits in patients with lesions to the right hippocampus and to the right parahippocampal cortex. *Neuropsychologia.* 36:1217–1238.
- Burgess N, Maguire EA, O'Keefe J. 2002. The human hippocampus and spatial and episodic memory. *Neuron.* 35:625–641.
- Castellanos FX, Giedd JN, Marsh WL, Hamburger SD, Vaituzis AC, Dickstein DP, Sarfatti SE, Vauss YC, Snell JW, Lange N *et al.* 1996. Quantitative brain magnetic resonance imaging in attention-deficit hyperactivity disorder. *Arch Gen Psychiatry.* 53(7):607–616.
- Castellanos FX, Lee PP, Sharp W, Jeffries NO, Greenstein DK, Clasen LS, Blumenthal JD, James RS, Ebens CL, Walter JM *et al.* 2002. Developmental trajectories of brain volume abnormalities in

- children and adolescents with attention-deficit/hyperactivity disorder. *J Am Med Assoc.* 288(14):1740–1748.
- Cauda F, Geda E, Sacco K, D'Agata F, Duca S, Geminiani G, Keller R. 2011. Grey matter abnormality in autism spectrum disorder: An activation likelihood estimation meta-analysis study. *J Neurol Neurosurg Psychiatry.* 82(12):1304–1313.
- Caviness VS, Filipek PA, Kennedy DN. 1989. Magnetic resonance technology in human brain science: Blueprint for a program based upon morphometry. *Brain Dev.* 11(1):1–13.
- Caviness VS, Kennedy DN, Bates JF, Makris N. 1996. The developing brain: A morphometric profile. In: Thatcher RW, Lyon GR, Rumsey J, Krasnegor N, editors. *Developmental neuroimaging: Mapping the development of brain and behavior.* New York: Academic Press. p. 3–14.
- Caviness VS, Kennedy DN, Richelme C, Rademacher J, Filipek PA. 1996. The human brain age 7–11 years: A volumetric analysis based on magnetic resonance images. *Cerebral Cortex.* 6(5):726–736.
- Caviness VS, Meyer J, Makris N, Kennedy DN. 1996. MRI-based topographic parcellation of human neocortex: An anatomically specified method with estimate of reliability. *J Cogn Neurosci.* 8:556–587.
- Center for Morphometric Analysis (CMA), segmentation manual. Massachusetts General Hospital (MGH). 2004. <http://www.cma.mgh.harvard.edu/manuals/segmentation/>.
- Ciesielski KT, Harris RJ, Hart BL, Pabst HF. 1997. Cerebellar hypoplasia and frontal lobe cognitive deficits in disorders of early childhood. *Neuropsychologia.* 35(5):643–655.
- Courchesne E, Karns CM, Davis HR, Ziccardi R, Carper RA, Tigue ZD, Chisum HJ, Moses P, Pierce K, Lord C et al. 2001. Unusual brain growth patterns in early life in patients with autistic disorder: An MRI study. *Neurology.* 57(2):245–254.
- Courchesne E, Saitoh O, Yeung-Courchesne R, Press GA, Lincoln AJ, Haas RH, Schreibman L. 1994. Abnormality of cerebellar vermian lobules VI and VII in patients with infantile autism: Identification of hypoplastic and hyperplastic subgroups with MR imaging. *AJR Am J Roentgenol.* 162(1):123–130.
- Courchesne E, Yeung-Courchesne R, Press GA, Hesselink JR, Jernigan TL. 1988. Hypoplasia of cerebellar vermal lobules VI and VII in autism. *N Engl J Med.* 318(21):1349–1354.
- Diedrichsen J, Balsters JH, Flavell J, Cussans E, Ramnani N. 2009. A probabilistic MR Atlas of the human cerebellum. *NeuroImage.* 46:39–46.
- Filipek PA, Kennedy DN. 1992. Neuroimaging in child neuropsychology. In: Boller F, Grafman J, editors. *Handbook of neuropsychology.* Vol. 6. Amsterdam: Elsevier. p. 301–329.
- Filipek PA, Kennedy DN, Caviness VS, Jr. 1991. Volumetric analyses of central nervous system neoplasm based on MRI. *Pediatr Neurol.* 7(5):347–351.
- Filipek PA, Kennedy DN, Caviness VS, Jr, Rossnick SL, Spraggins TA, Starewicz PM. 1989. Magnetic resonance imaging based brain morphometry: Development and application to normal subjects. *Ann Neurol.* 25(1):61–67.
- Filipek PA, Richelme C, Kennedy DN, Caviness VS, Jr. 1994. The young adult human brain: An MRI-based morphometric study. *Cereb Cortex.* 4(4):344–360.
- Gadian DG, Aicardi J, Watkins KE, Porter DA, Mishkin M, Vargha-Khadem F. 2000. Developmental amnesia associated with early hypoxic-ischaemic injury. *Brain.* 123(3):499–507.
- Galaburda AM, Rosen GD, Sherman GF. 1987. Individual variability in cortical organization: Its relationship to brain laterality and implications to function. *Neuropsychologia.* 28:529–546.
- Gale CR, O'Callaghan FJ, Bredow M, Martyn CN, Avon Longitudinal Study of Parents and Children Study Team. 2006. The influence of head growth in fetal life, infancy, and childhood on intelligence at the ages of 4 and 8 years. *Pediatrics.* 118(4):1486–1492.
- Giedd JN, Rapoport JL. 2010. Structural MRI of pediatric brain development: What have we learned and where are we going? *Neuron.* 67:728–734.
- Giedd JN, Snell JW, Lange N, Rajapakse JC, Casey BJ, Kozuch PL, Vaituzis AC, Vauss YC, Hamburger SD, Kayser D et al. 1996. Quantitative magnetic resonance imaging of human brain development: Ages 4–18. *Cereb Cortex.* 6(4):551–560.
- Giedd JN, Vaituzis AC, Hamburger SD, Lange N, Rajapakse JC, Kayser D, Vauss YC, Rapoport JL. 1996. Quantitative MRI of the temporal lobe, amygdala, and hippocampus in normal human development: Ages 4–18 years. *J Comp Neurol.* 366(2):223–230.
- Gilles FH, Leviton A, Dooling EC. 1983. *The developing human brain: Growth and epidemiologic neuropathology.* Boston, Bristol, London: John Wright PSG Inc.
- Gilmore JH, Lin W, Prastawa MW, Looney CB, Vetsa YS, Knickmeyer RC, Evans DD, Smith JK, Hamer RM, Lieberman JA et al. 2007. Regional gray matter growth, sexual dimorphism, and cerebral asymmetry in the neonatal brain. *J Neurosci.* 27(6):1255–1260.
- Gilmore JH, Shi F, Woolson SL, Knickmeyer RC, Short SJ, Lin W, Zhu H, Hamer RM, Styner M, Shen D. 2011. Longitudinal development of cortical and subcortical gray matter from birth to 2 years. *Cereb Cortex.* doi: 10.1093/cercor/bhr327.
- Glaser H, Leroy F, Dubois J, Hertz-Pannier L, Mangin JF, Dehaene-Lambertz G. 2011. A robust cerebral asymmetry in the infant brain: The rightward superior temporal sulcus. *NeuroImage.* 58(3):716–723.
- Gompertz B. 1825. On the nature of the function expressive of the law of human mortality, and on a new mode of determining the value of life contingencies. *Philos Trans R Soc Lond.* 115:513–585.
- Good CD, Johnsrude I, Ashburner J, Henson RN, Friston KJ, Frackowiak RS. 2001. Cerebral asymmetry and the effects of sex and handedness on brain structure: A voxel-based morphometric analysis of 465 normal adult human brains. *NeuroImage.* 14(3):685–700.
- Gunning-Dixon FM, Head D, McQuain J, Acker JD, Raz N. 1998. Differential aging of the human striatum: A prospective MR imaging study. *AJNR Am J Neuroradiol.* 19(8):1501–1507.
- Haznedar MM, Buchsbaum MS, Wei TC, Hof PR, Cartwright C, Bienstock CA, Hollander E. 2000. Limbic circuitry in patients with autism spectrum disorders studied with positron emission tomography and magnetic resonance imaging. *Am J Psychiatry.* 157(12):1994–2001.
- Herbert MR, Ziegler DA, Deutsch CK, O'Brien LM, Lange N, Bakardjieva A, Hodgson J, Adrien KT, Steele S, Makris N, Jr et al. 2003. Dissociations of cerebral cortex, subcortical and cerebral white matter volumes in autistic boys. *Brain.* 126(Pt 5):1182–1192.
- Holland BA, Haas DK, Norman D, Brant-Zawadzki M, Newton TH. 1986. MRI of normal brain maturation. *AJNR Am J Neuroradiol.* 7(2):201–208.
- Hollingshead AB. 1975. The four-factor index of social status. New Haven, CT: Department of Sociology, Yale University.
- Hu D, Shen H, Zhou Z. 2008. Functional asymmetry in the cerebellum: A brief review. *Cerebellum.* 7(3):304–313.
- Huppi PS, Warfield S, Kikinis R, Barnes PD, Zientara GP, Jolesz FA, Tsuji MK, Volpe JJ. 1998. Quantitative magnetic resonance imaging of brain development in premature and mature newborns. *Ann Neurol.* 43:224–235.
- Ifthikharuddin SF, Shrier DA, Numaguchi Y, Tang X, Ning R, Shibata DK, Kurlan R. 2000. MR volumetric analysis of the human basal ganglia: Normative data. *Acad Radiol.* 7(8):627–634.
- Isaacs EB, Vargha-Khadem F, Watkins KE, Lucas A, Mishkin M, Gadian DG. 2003. Developmental amnesia and its relationship to degree of hippocampal atrophy. *Proc Natl Acad Sci USA.* 100(22):13060–13063.
- Jack CR, Jr, Twomey CK, Zinsmeister AR, Sharbrough FW, Petersen RC, Cascino GD. 1989. Anterior temporal lobes and hippocampal formations: Normative volumetric measurements from MR images in young adults. *Radiology.* 172(2):549–554.
- Kasprian G, Langs G, Brugge PC, Bittner M, Weber M, Arantes M, Prayer D. 2011. The prenatal origin of hemispheric asymmetry: An in utero neuroimaging study. *Cereb Cortex.* 21:1076–1083.
- Kaufmann WE, Cooper KL, Mostofsky SH, Capone GT, Kates WR, Newschaffer CJ, Bukelis I, Stump MH, Jann AE, Lanham DC. 2003. Specificity of cerebellar vermian abnormalities in autism: A quantitative magnetic resonance imaging study. *J Child Neurol.* 18(7):463–470.

- Kennedy DN. 1986. A system of three-dimensional analysis of magnetic resonance images. Cambridge, MA: Department of Nuclear Engineering, Massachusetts Institute of Technology.
- Kennedy DN, Filippek PA. 1989. Anatomic segmentation and volumetric analysis in nuclear magnetic resonance imaging. *IEEE Trans Med Imag.* 7:1–7.
- Kennedy DN, Meyer J. 1994. MRI-based topographic segmentation. In: Thatcher W, Hallet M, Zepffiro T, John R, Huerta M, editors. *Functional neuroimaging: Technical foundations*. New York: Academic Press. p. 201–208.
- Kennedy DN, Nelson AC. 1987. Three-dimensional display from cross-sectional tomographic images: An application to magnetic resonance imaging. *IEEE Trans Med Imag.* 6:134–141.
- Kliegman RM, Behrman RE, Jenson HB, Santon BF. 2007. *Nelson textbook of pediatrics*. 18th edition. Philadelphia, PA: Saunders. p. 135.
- Knickmeyer RC, Gouttard S, Kang C, Evans D, Wilber K, Smith JK, Hamer RM, Lin W, Gerig G, Gilmore JH. 2008. A structural MRI study of human brain development from birth to 2 years. *J Neurosci.* 28(47):12176–12182.
- Lenroot RK, Gogtay N, Greenstein DK, Wells EM, Wallace GL, Clasen LS, Blumenthal JD, Lerch J, Zijdenbos AP, Evans AC et al. 2007. Sexual dimorphism of brain developmental trajectories during childhood and adolescence. *Neuroimage.* 36:1065–1073.
- Levitt J, Blanton R, Capetillo-Cunliffe L, Guthrie D, Toga A, McCracken J. 1999. Cerebellar vermis lobules VIII–X in autism. *Prog Neuropsychopharmacol Biol Psychiatry.* 23(4):625–633.
- Li YJ, Ga SN, Huo Y, Li SY, Gao XG. 2007. Characteristics of hippocampal volumes in healthy Chinese from MRI. *Neurol Res.* 29 (8):803–806.
- Liu WC, Flax JF, Guise KG, Sukul V, Benasich AA. 2008. Functional connectivity of the sensorimotor area in naturally sleeping infants. *Brain Res.* 1223:42–49.
- Looi JC, Lindberg O, Zandbelt BB, Ostberg P, Andersen C, Botes L, Svensson L, Wahlund LO. 2008. Caudate nucleus volumes in frontotemporal lobar degeneration: Differential atrophy in subtypes. *AJNR Am J Neuroradiol.* 29(8):1537–1543.
- Madsen SK, Ho AJ, Hua X, Saharan PS, Toga AW, Jack CR, Jr, Weiner MW, Thompson PM, The Alzheimer's Disease Neuroimaging Initiative. 2010. 3D maps localize caudate nucleus atrophy in 400 Alzheimer's disease, mild cognitive impairment, and healthy elderly subjects. *Neurobiol Aging.* 31(8):1312–1325.
- Makris N, Meyer JW, Bates JF, Yeterian EH, Kennedy DN, Caviness VS. 1999. MRI-Based topographic parcellation of human cerebral white matter and nuclei II. Rationale and applications with systematics of cerebral connectivity. *Neuroimage.* 9(1):18–45.
- Martin RD. 1983. Human brain evolution in an ecological context. 52nd James Arthur Lecture. New York: American Museum of Natural History.
- Matsuzawa J, Matsui M, Konishi T, Noguchi K, Gur RC, Bilker W, Miyawaki T. 2001. Age-related volumetric changes of brain gray and white matter in healthy infants and children. *Cereb Cortex.* 11 (4):335–342.
- McArdle CB, Richardson CJ, Nicholas DA, Mirfakhraee M, Hayden CK, Amparo EG. 1987. Developmental features of the neonatal brain: MR imaging. Part I. Gray-white matter differentiation and myelination. *Radiology.* 162(1 Pt 1):223–229.
- Meyer J, Makris N, Bates JF, Caviness VS, Kennedy DN. 1999. MRI-Based topographic parcellation of the human cerebral white matter: I. Technical foundations. *Neuroimage.* 9:1–17.
- Miyawaki T, Matsui K, Takashima S. 1998. Developmental characteristics of vessel density in the human fetal and infant brains. *Early Human Dev.* 53(1):65–72.
- Munson J, Dawson G, Abbott R, Faja S, Webb SJ, Friedman SD, Shaw D, Artru A, Dager SR. 2006. Amygdala volume and behavioral development in autism. *Arch Gen Psychiatry.* 63:686–693.
- Nishida M, Makris N, Kennedy DN, Vangel M, Fischl B, Krishnamoorthy KS, Caviness VS, Grant PE. 2006. Detailed semi-automated MRI based morphometry of the neonatal brain: Preliminary results. *Neuroimage.* 32:1041–1049.
- Nopoulos P, Flaum M, O'Leary D, Andreasen NC. 2000. Sexual dimorphism in the human brain: Evaluation of tissue volume, tissue composition and surface anatomy using magnetic resonance imaging. *Psychiatry Res.* 98(1):1–13.
- Ortiz-Mantilla S, Choe MS, Flax J, Grant PE, Benasich AA. 2010. Associations between the size of the amygdala in infancy and language abilities during the preschool years in normally developing children. *Neuroimage.* 49(3):2791–2799.
- Ostby Y, Tamnes CK, Fjell AM, Westlye LT, Due-Tønnessen P, Walhovd KB. 2009. Heterogeneity in subcortical brain development: A structural magnetic resonance imaging study of brain maturation from 8 to 30 years. *J Neurosci.* 29(38):11772–11782.
- Packard MG, Knowlton BJ. 2002. Learning and memory functions of the basal ganglia. *Annu Rev Neurosci.* 25(1):563–593.
- Pangelinan MM, Zhang G, VanMeter JW, Clark JE, Hatfield BD, Hafler AJ. 2011. Beyond age and gender: Relationships between cortical and subcortical brain volume and cognitive-motor abilities in school-age children. *Neuroimage.* 54(4):3093–3100.
- Paterson SJ, Badridze N, Flax JF, Liu WC, Benasich AA. 2004. A protocol for structural MRI scanning of non-sedated infants. *Proc J Cogn Neurosci.* 15:F124.
- Paus T, Collins DL, Evans AC, Leonard G, Pike B, Zijdenbos A. 2001. Maturation of white matter in the human brain: A review of magnetic resonance studies. *Brain Res Bull.* 54(3):255–266.
- Pfefferbaum A, Mathalon DH, Sullivan EV, Rawles JM, Zipursky RB, Lim KO. 1994. A quantitative magnetic resonance imaging study of changes in brain morphology from infancy to late adulthood. *Arch Neurol.* 51(9):874–887.
- Pfluger T, Weil S, Weis S, Vollmar C, Heiss D, Egger J, Scheck R, Hahn K. 1999. Normative volumetric data of the developing hippocampus in children based on magnetic resonance imaging. *Epilepsia.* 40(4):414–423.
- Rademacher J, Galaburda AM. 1992. Human cerebral cortex: Localization, parcellation, and morphometry with magnetic resonance imaging. *J Cogn Neurosci.* 4:352–374.
- Raschle N, Zuk J, Ortiz-Mantilla S, Sliva D, Fraceschi A, Grant PE, Benasich AA, Gaab N. 2012. Pediatric neuroimaging in early childhood and infancy: Challenges and practical guidelines. *Ann N Y Acad Sci.* 1252(1):43–50.
- Raz N, Gunning-Dixon F, Head D, Rodrigue KM, Williamson A, Acker JD. 2004. Aging, sexual dimorphism, and hemispheric asymmetry of the cerebral cortex: Replicability of regional differences in volume. *Neurobiol Aging.* 25(3):377–396.
- Raz N, Torres JJ, Acker JD. 1995. Age, gender, and hemispheric differences in human striatum: A quantitative review and new data from in vivo MRI morphometry. *Neurobiol Learn Mem.* 63 (2):133–142.
- Reiss AL, Abrams MT, Singer HS, Ross JL, Denckla MB. 1996. Brain development, gender and IQ in children. A volumetric imaging study. *Brain.* 119:1763–1774.
- Rudie JD, Shehzad Z, Hernandez LM, Colich NL, Bookheimer SY, Iacoboni M, Dapretto M. 2012. Reduced functional integration and segregation of distributed neural systems underlying social and emotional information processing in autism spectrum disorders. *Cereb Cortex.* 22(5):1025–1037.
- Schmahmann JD, Weilburg JB, Sherman JC. 2007. The neuropsychiatry of the cerebellum—insights from the clinic. *Cerebellum.* 6 (3):254–267.
- Shaw P, Kabani NJ, Lerch JP, Eckstrand K, Lenroot R, Gogtay N, Greenstein D, Clasen L, Evans A, Rapoport JL et al. 2008. Neurodevelopmental trajectories of the human cerebral cortex. *J Neurosci.* 28:3586–3594.
- Shi F, Yap PT, Wu G, Jia H, Gilmore JH, Lin W, Shen D. 2011. Infant brain atlases from neonates to 1- and 2-year-olds. *PLoS One.* 6(4):e18746.
- Sowell ER, Jernigan TL. 1998. Further MRI evidence of late brain maturation: Limbic volume increases and changing asymmetries during childhood and adolescence. *Dev Neuropsychol.* 14 (4):599–617.
- Stoodley CJ, Schmahmann JD. 2009. Functional topography in the human cerebellum: A meta-analysis of neuroimaging studies. *NeuroImage.* 44:489–501.

- Sun T, Walsh CA. 2006. Molecular approaches to brain asymmetry and handedness. *Nat Rev Neurosci.* 7:655–662.
- Szabó CA, Lancaster JL, Xiong J, Cook C, Fox P. 2003. MR Imaging volumetry of subcortical structures and cerebellar hemispheres in normal persons. *AJNR Am J Neuroradiol.* 24:644–647.
- Szatmari P, Offord DR, Boyle MH. 1989. Ontario Child Health Study: Prevalence of attention deficit disorder with hyperactivity. *J Child Psychol Psychiatry.* 30(2):219–230.
- Takashima S, Itoh M, Oka A. 2009. A history of our understanding of cerebral vascular development and pathogenesis of perinatal brain damage over the past 30 years. *Semin Pediatr Neurol.* 16 (4):226–236.
- Thompson DK, Wood SJ, Doyle LW, Warfield SK, Egan GF, Inder TE. 2009. MR-determined hippocampal asymmetry in full-term and preterm neonates. *Hippocampus.* 19(2):118–123.
- Tiemeier H, Lenroot RK, Greenstein DK, Tran L, Pierson R, Giedd JN. 2010. Cerebellum development during childhood and adolescence: A longitudinal morphometric MRI study. *Neuroimage.* 49 (1):63–70.
- Toga AW, Thompson PM. 2003. Mapping brain asymmetry. *Nat Rev Neurosci.* 4:37–48.
- Utsunomiya H, Takano K, Okazaki M, Mitsudome A. 1999. Development of the temporal lobe in infants and children: Analysis by MR-based volumetry. *Am J Neuroradiol.* 20(4):717–723.
- van der Knaap MS, Valk J. 1990. MR imaging of the various stages of normal myelination during the first year of life. *Neuroradiology.* 31(6):459–470.
- Volpe JJ. 2009. Cerebellum of the premature infant: Rapidly developing, vulnerable, clinically important. *J Child Neurol.* 24 (9):1085–1104.
- Wang L, LaViolette P, O'Keefe K, Putcha D, Bakkour A, Van Dijk KRA, Pihlajamäki M, Dickerson BC, Sperling RA. 2010. Intrinsic connectivity between the hippocampus and posteromedial cortex predicts memory performance in cognitively intact older individuals. *NeuroImage.* 51:910–917.
- Wang L, Shi F, Lin W, Gilmore JH, Shen D. 2011. Automatic segmentation of neonatal images using convex optimization and coupled level sets. *Neuroimage.* 58:805–817.
- Watkins KE, Paus T, Lerch JP, Zijdenbos A, Collins DL, Neelin P, Taylor J, Worsley KJ, Evans AC. 2001. Structural asymmetries in the human brain: A voxel-based statistical analysis of 142 MRI scans. *Cereb Cortex.* 11(9):868–877.
- Webb SJ, Sparks BF, Friedman SD, Shaw DW, Giedd J, Dawson G, Dager SR. 2009. Cerebellar vermal volumes and behavioral correlates in children with autism spectrum disorder. *Psychiatry Res.* 172(1):61–67.
- Wellington TM, Semrud-Clikeman M, Gregory AL, Murphy JM, Lancaster JL. 2006. Magnetic resonance imaging volumetric analysis of the putamen in children with ADHD: Combined type versus control. *J Atten Disord.* 10(2):171–180.
- Worth AJ, Makris N, Caviness VS, Jr, Kennedy DN. 1997. Neuroanatomical segmentation in MRI: Technological objectives. *Int J Pattern Recogn Artif Intell.* 11:1161–1187.
- Worth AJ, Makris N, Meyer JW, Caviness VS, Jr, Kennedy DN. 1997. Automated segmentation of brain exterior in MR images driven by empirical procedures and anatomical knowledge. International Conference on Information Processing in Medical Imaging; Poultney, Vermont.
- Yamashita K, Yoshiura T, Hiwatashi A, Noguchi T, Togao O, Takayama Y, Nagao E, Kamano H, Hatakenaka M, Honda H. 2011. Volumetric asymmetry and differential aging effect of the human caudate nucleus in normal individuals: A prospective MR imaging study. *J Neuroimaging.* 21(1):34–37.
- Ystad MA, Lundervold AJ, Wehling E, Espeseth T, Rootwelt H, Westlye LT, Andersson M, Adolfsdottir S, Geitung JT, Fjell AM et al. 2009. Hippocampal volumes are important predictors for memory function in elderly women. *BMC Med Imaging.* 9:17.
- Yu X, Zhang Y, Lasky RE, Datta S, Parikh NA, Narayana PA. 2010. Comprehensive brain MRI segmentation in high risk preterm newborns. *PLoS One.* 5(11):e13874.